The Company of **Biologists**

SPECIAL ISSUE: CELL BIOLOGY OF THE IMMUNE SYSTEM

RPTPε promotes M2-polarized macrophage migration through ROCK2 signaling and podosome formation

Fanny Lapointe[1], Sylvie Turcotte[1], Joanny Roy[2], Elyse Bissonnette[2], Marek Rola-Pleszczynski[1] and Jana Stankova[1,*]

ABSTRACT

Cysteinyl-leukotrienes (cys-LTs) have well-characterized physiopathological roles in the development of inflammatory diseases. We have previously found that protein tyrosine phosphatase ε (PTPε) is a signaling partner of CysLT$_1$R, a high affinity receptor for leukotriene D4 (LTD$_4$). There are two major isoforms of PTPε, receptor-like (RPTPε) and cytoplasmic (cyt-)PTPε, both of which are encoded by the *PTPRE* gene but from different promoters. In most cells, their expression is mutually exclusive, except in human primary monocytes, which express both isoforms. Here, we show differential PTPε isoform expression patterns between monocytes, M1 and M2 human monocyte-derived macrophages (hMDMs), with the expression of glycosylated forms of RPTPε predominantly in M2-polarized hMDMs. Using PTPε-specific siRNAs and expression of RPTPε and cyt-PTPε, we found that RPTPε is involved in monocyte adhesion and migration of M2-polarized hMDMs in response to LTD$_4$. Altered organization of podosomes and higher phosphorylation of the inhibitory Y-722 residue of ROCK2 was also found in PTPε-siRNA-transfected cells. In conclusion, we show that differentiation and polarization of monocytes into M2-polarized hMDMs modulates the expression of PTPε isoforms and RPTPε is involved in podosome distribution, ROCK2 activation and migration in response to LTD$_4$.

KEY WORDS: Protein tyrosine phosphatase ε, M2-polarized macrophages, Migration, Podosomes, ROCK2, Leukotriene

INTRODUCTION

Macrophages are a crucial component of the innate immune system and their presence throughout the various tissues of the organism is fundamental to homeostasis. They clear pathogens, heal damaged tissues and regulate multiple immune and inflammatory responses. However, excessive infiltration and activation of macrophages may destabilize this precarious equilibrium and exacerbate pathological processes, such as neurodegenerative diseases, metabolic syndromes, cancer development and chronic inflammatory disorders, such as allergic asthma (Schultze et al., 2015; Wynn et al., 2013).

In the particular context of asthma, where the airways are continuously challenged by a variety of foreign substances, alveolar macrophages (AMs), located on the alveolar epithelial surface, have the ability to maintain physiological homeostasis of the lungs by tempering allergic inflammation (Mayernik et al., 1983; Toews et al.,

1984; Gant et al., 1992). Under an allergic challenge, resident AMs proliferate locally (Jenkins et al., 2011) or differentiate from interstitial macrophages (IMs), located within alveolar walls (Thomas et al., 1976; Landsman and Jung, 2007), and constrain allergic airway inflammation, thus sustaining homeostasis. However, when inflammation is established, polarized AMs represent a continuum of activation phenotypes (Murray et al., 2014; Xue et al., 2014), losing their homeostatic commitment and gaining pathogenic functions. Indeed, higher numbers of M2 macrophages are found in bronchial alveolar lavage from asthmatic patients when compared with healthy subjects (Girodet et al., 2016; Draijer et al., 2013, 2017), and in mice challenged with house dust mites (Lee et al., 2015). Additionally, lung-recruited monocytes have been shown to exacerbate the perceived allergic reaction (Zasłona et al., 2014; Lee et al., 2015). Regulation of migration of macrophage precursors may thus be seen as a therapeutic objective in order to facilitate the resolution of inflammation and to re-establish immune homeostasis in these patients.

Cysteinyl-leukotrienes (Cys-LTs), which comprise LTC$_4$, LTD$_4$ and LTE$_4$, are potent inflammatory mediators and have well-characterized pathophysiological roles in the development and progression of asthma, including inflammatory cell recruitment (Hay et al., 1995). For instance, LTD$_4$, via its high affinity receptor, CysLT$_1$R (Lynch et al., 1999), induces myeloid cell chemotaxis (Thivierge et al., 2001, 2006, 2009) and cytoskeleton rearrangement through Rho signaling (Saegusa et al., 2001; Massoumi et al., 2002). Of note, CysLT$_1$R antagonists are widely used in allergic asthma treatment (Scott and Peters-Golden, 2013).

In order to enter the alveolar space during allergic inflammation, recruited monocytes must get through the vasculature and the interstitial pulmonary tissues (Landsman and Jung, 2007) using a succession of migration movements. The type of physical barrier by which a cell is confronted dictates the migration mechanism that will be employed (Van Goethem et al., 2010, 2011; Guiet et al., 2011). Hence, monocytes, at first, can slip through a porous matrix using amoeboid-type migration. Defined by a round cell shape and the absence of robust adherence, this first migration type is mostly used by leukocytes. Macrophages, on the other hand, are unique among leukocytes in being able to use proteolysis to break through denser tissues (Van Goethem et al., 2010; Guiet et al., 2011), with long membrane protrusions and strong integrin interactions that define a mesenchymal-type migration (Cougoule et al., 2012). These two migration processes are divergent in their signaling pathways, as amoeboid migration is Rho kinase (ROCK)-dependent, whereas mesenchymal migration is enhanced following ROCK inhibition (Gui et al., 2014).

ROCK, a serine/threonine kinase, is among the best-characterized downstream effector of the Rho family of small GTPases. Two isoforms of the kinase have been identified so far – ROCK1 and ROCK2 – and both are activated by various mechanisms: autologous

[1]Division of Immunology and Allergy, Department of Pediatrics, Faculty of Medicine and Health Sciences, Université de Sherbrooke, Sherbrooke, Quebec J1H 5N4, Canada. [2]Department of Medicine, Université Laval, Québec G1V 4G5, Canada.

*Author for correspondence (Jana.Stankova@USherbrooke.ca)

J.R., 0000-0002-5169-3594; J.S., 0000-0002-4127-8506

binding of the C-terminus (Amano et al., 1997, 1999), conformational change induced by RhoA binding (Matsui et al., 1996; Doran et al., 2004), binding of lipid messengers (Feng et al., 1999), proteolytic cleavage (Sebbagh et al., 2001, 2005) and phosphorylation (Lowery et al., 2007; Lee and Chang, 2008; Lee et al., 2010; Pan et al., 2013; Chuang et al., 2012, 2013). However, phosphorylation of the residue Tyr-722 of ROCK2 is considered inhibitory as it prevents RhoA-mediated ROCK2 activation and adds an additional regulatory step in ROCK2-induced myosin light chain phosphorylation (Amano et al., 1996; Kawano et al., 1999). The actomyosin system is necessary to generate the contractile force and cytoskeleton reorganization essential for pleiotropic cellular processes, including apoptosis and proliferation, but is also necessary for the rounding and adhesion mechanisms guiding amoeboid cell migration (Amano et al., 2010). On the other hand, mesenchymal migration, facilitated by podosomes (Calle et al., 2006; Carman et al., 2007), is impeded by excessive ROCK signaling, causing an actomyosin-dependent disassembly of these specialized punctate adhesion structures (Kuo et al., 2018; Yu et al., 2013; van Helden et al., 2008; Pan et al., 2011).

Podosomes have long been described as part of the primary adhesion machinery of macrophages, but they are formed by most cells of the myeloid lineage (Linder, 2007). As specialized adhesion structures, podosomes are microscopically defined as F-actin-rich dots surrounded by a ring of cytoskeletal proteins connecting integrins to the actin cytoskeleton (Linder, 2007). They are found either isolated or arranged in superstructures, such as clusters, rosettes or belts, and are interconnected through a network of actin filaments (Panzer et al., 2016; Luxenburg et al., 2007; Bhuwania et al., 2012). Regulation of these filaments is crucial for the optimal actomyosin tractive force required for cell migration (Collin et al., 2008; van den Dries et al., 2013; Evans et al., 2003).

A major regulator of podosome arrangement in osteoclasts is the protein tyrosine phosphatase ε (PTPε) (Chiusaroli et al., 2004; Granot-Attas et al., 2009; Finkelshtein et al., 2014). In these cells, the podosome belt structure is crucial for efficient bone resorption and PTPε regulates ROCK activity, thus leading to proper assembly, dynamics, and subcellular organization of these podosomes (Granot-Attas et al., 2009; Chiusaroli et al., 2004). Accordingly, *Ptpre$^{-/-}$* (hereafter PTPε$^{-/-}$) mice exhibit an increase in bone mass, which coincides with defective osteoclast bone adhesion and resorption as a consequence of disorganized podosomes.

PTPε is represented by five different isoforms (all of which are encoded by a single *PTPRE* gene); the receptor-type (RPTPε), which presents multiple glycosylated forms depending on its two extracellular asparagine residues (Asn-23, Asn-30), and four non-transmembrane, cytoplasmic (cyt)-PTPε isoforms [cyt-PTPε, p67 (Gil-Henn et al., 2000), p65 (Gil-Henn et al., 2001) and cyt-PTPεD1 (Wabakken et al., 2002)]. RPTPε and cyt-PTPε are the most abundantly expressed and are generated by the use of alternative promoters (Tanuma et al., 1999). RPTPε has two putative glycosylation sites. The role of the glycosylated form of RPTPε has not been directly studied; however, Berman-Golan and Elson (Berman-Golan and Elson, 2007) observed that in mammary tumor cells it was only the glycosylated form of RPTPε that was phosphorylated by Neu (also known as ERBB2) and thus could activate Src.

In the majority of murine cell types examined, cyt-PTPε and RPTPε expression is mutually exclusive (Elson and Leder, 1995). However, we have previously shown that both isoforms are expressed in human primary monocytes (Lapointe et al., 2019). Their divergent pattern of expression in polarized human

monocyte-derived macrophages (hMDMs) is the focus of the present study.

Here, we present a characteristic expression pattern of RPTPε in M2-polarized hMDMs. We also examine the involvement of this isoform in migration, through the regulation of ROCK2 Tyr-722 phosphorylation and podosome arrangement. Moreover, we show that mutation of the putative N-glycosylated Asn-23 residue of RPTPε results in increased ROCK2 Tyr-722 phosphorylation.

RESULTS

cyt-PTPε and RPTPε expression is differentially modulated by cytokines in human primary monocytes

Regulation of PTPε expression has not been fully studied in human cells. However, unlike rat and murine cells, human primary monocytes express cyt-PTPε and RPTPε simultaneously (Lapointe et al., 2019). To follow up on this observation, we were interested in examining the modulation of expression of PTPε isoforms in these cells as they are the precursors of hMDMs *in vitro* and macrophages *in vivo*.

We have previously shown that cyt-PTPε and RPTPε were involved in LTD$_4$-induced CysLT$_1$R signaling (Lapointe et al., 2019) with cyt-PTPε having the predominant role in IL-8 production. Here, we first studied the effect of LTD$_4$ on cyt-PTPε and RPTPε expression. By quantitative real-time PCR (RT-qPCR), we showed a slight upregulation of *cyt-PTPε* mRNA expression following LTD$_4$ stimulation (Fig. 1A). Cyt-PTPε protein expression was significantly upregulated following a 24-h stimulation, as demonstrated by western blot densitometry analysis (Fig. 1B).

We also examined the regulation of PTPε by cytokines that are important in the pathophysiologic context of asthma. In lung inflammation, in addition to cys-LTs, multiple Th2 polarizing cytokines are secreted and could modulate PTPε expression. Given that some of these cytokines are used in the polarization protocols for hMDMs, it was important to determine if they had direct effects on PTPε expression. Fig. 1C,D shows an upregulation of *cyt-PTPε* mRNA and cyt-PTPε protein expression with IL-4 stimulation. Intriguingly, a similar pattern of PTPε upregulation was seen with both IL-4 and LTD$_4$ stimulation. Since it had been shown that IL-4 can upregulate cys-LT synthesis (Hsieh et al., 2001), we investigated the potential involvement of cys-LTs in IL-4-stimulated upregulation of *PTPε* mRNA expression. When monocytes were pretreated with a leukotriene synthesis inhibitor (MK886), IL-4-induced upregulation of *PTPε* mRNA expression was completely abolished (Fig. 1E). The Th2 cytokines IL-13 and IL-5, on the other hand, had no modulatory effect on PTPε expression (Fig. S1A,B). Moreover, no involvement of these cytokines has been noted in cys-LT production.

We also examined whether pro-inflammatory cytokines, which may be involved in Th1 polarization, could also modulate PTPε expression. As presented in Fig. 2A,B, a time-dependent upregulation of *cyt-PTPε* mRNA was observed following IFNγ stimulation. A significant upregulation of cyt-PTPε protein expression was also seen after a 24-h stimulation. Interestingly, the expression of both cyt-PTPε and RPTPε was upregulated with IL-1β stimulation (Fig. 2C); however, TNFα did not modulate their expression (Fig. S1C).

Polarization differentially modulates PTPε expression in hMDM

Alveolar macrophages represent a large proportion of the immune cells of the lung and arise from local proliferation or differentiation of monocyte precursors (Thomas et al., 1976; Landsman and Jung, 2007; Jenkins et al., 2011). In asthma, they polarize to a M2 subtype
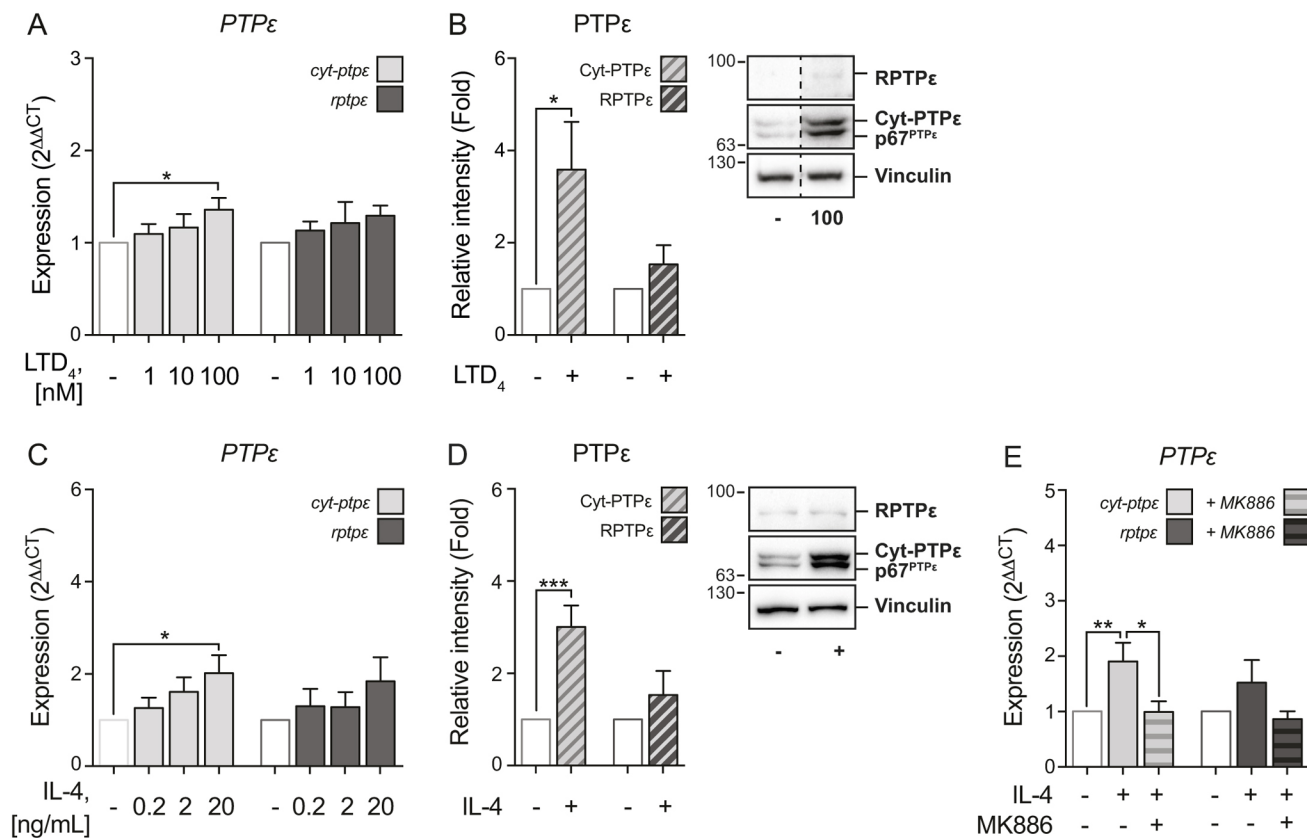
Fig. 1. Cys-LT-dependent increases of cyt-PTPε expression by IL-4 stimulation in human primary monocytes. Human primary monocytes were stimulated with LTD_4 or IL-4, as indicated. Following a 3-h stimulation with (A) LTD_4 (or its vehicle, EtOH) or (C) IL-4, at the indicated concentrations, *cyt-PTPε* and *RPTPε* mRNA expression was analyzed by RT-qPCR and expressed as $2^{\Delta\Delta CT}$ over *GAPDH* mRNA expression (A, $n=20$; C, $n=6-9$). Following a 24-h stimulation with (B) LTD_4 (100 nM) (or its vehicle, EtOH) or (D) IL-4 (20 ng/ml), cyt-PTPε and RPTPε protein expression was analyzed by western blot densitometry quantification and expressed as relative intensity corrected for vinculin expression. Representative western blots are shown; dotted lines indicate where the image of the membrane has been modified to remove lanes irrelevant to the result (B: $n=23$, D: $n=12$). Control lanes in D are also used in Fig. 2B. (E) To study the role of endogenous cys-LTs in *cyt-PTPε* and *RPTPε* mRNA expression, MK886 (200 nM) was incubated with monocytes before a 3-h stimulation with IL-4 (20 ng/ml) and *cyt-PTPε* and *RPTPε* mRNA expression was quantified as previously described ($n=7$). Data are expressed as mean ±s.e.m. *$P<0.05$, **$P<0.005$, ***$P<0.001$, by (A,C) one-way ANOVA with Dunnett's multiple comparisons post-test to unstimulated condition, (B,D) Wilcoxon test, and (E) one-way ANOVA with Tukey's multiple comparisons post-test.

(Girodet et al., 2016; Draijer et al., 2013, 2017). Since polarizing cytokines regulated PTPε expression in primary monocytes, we examined whether differentiation and polarization of hMDMs would further modulate PTPε expression.

hMDMs were obtained following the described differentiation protocol and the expression of *CD11b*, *CD36* and *CD68* mRNA (macrophage differentiation markers) were analyzed by RT-qPCR to ascertain the differentiation state of the cells (Fig. S2A–C). hMDMs were then polarized using either IL-4 or the combination of IFNγ and lipopolysaccharide (LPS) as post-differentiation stimuli (Murray et al., 2014). These polarized macrophages, referred to as M2 and M1, respectively, were distinguishable by their phenotypic appearance, membrane receptors and chemokine gene expression. M1-polarized hMDMs presented a rounded shape and high expression of *IL-15Rα* and *CXCL11* mRNA, whereas M2-polarized hMDMs were elongated with ruffled membrane protrusions and showed high expression of *MRC-1* and *CCL22* mRNA, which correlates with what has been previously published (Martinez et al., 2006) (Fig. S2D–H).

As shown in Fig. 3A, RT-qPCR on M1-polarized hMDMs revealed increased *cyt-PTPε* mRNA expression compared to that in non-polarized hMDMs (Mφ). In contrast, *RPTPε* mRNA expression was significantly decreased with M1 polarization with no change with M2 polarization. However, western blot densitometry analysis showed a

different PTPε protein expression pattern. Quantification of cyt-PTPε and RPTPε protein expression in polarized hMDMs demonstrated the upregulation of cyt-PTPε only in M2-polarized hMDMs (Fig. 3B). Moreover, cyt-PTPεPD1 expression, a splice form of cyt-PTPε, found only in monocytic cells (Wabakken et al., 2002) and previously identified in human monocytes according to its predicted molecular mass (Lapointe et al., 2019), was significantly upregulated in M1-polarized hMDMs (Fig. 3C). As for RPTPε, a reduced expression was found in M1-polarized hMDMs, whereas a trend towards a higher expression of the glycosylated form of RPTPε (gly-RPTPε) (Fig. S3) was found in M2-polarized hMDMs. Interestingly, the glycosylated forms of gly-RPTPε were predominantly found in M2-polarized hMDMs and this post-translational modification was not observed in monocytes.

PTPε is involved in cell adhesion

Given that PTPε is important for osteoclast adhesion and that monocytes must be recruited to the inflammatory environment of the lung to differentiate into macrophages, we examined whether monocyte adhesion could modulate PTPε expression (Gerhardt and Ley, 2015).

Here, we show that monocyte adhesion considerably increased PTPε expression. A significant upregulation of PTPε was observed in
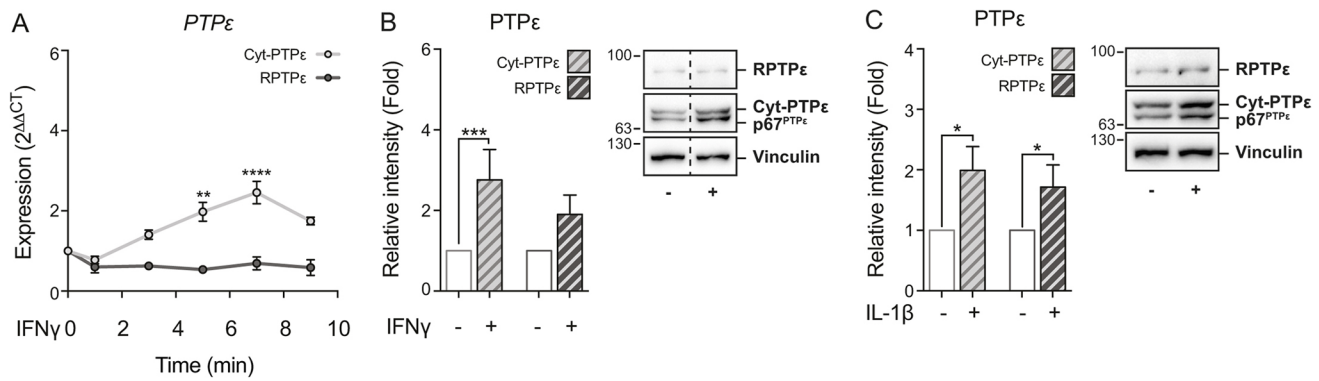
Fig. 2. Increase of PTPε expression after stimulation with IFNγ and IL-1β in human primary monocytes. Human primary monocytes were stimulated with IFNγ or IL-1β, as indicated. (A) Following the indicated stimulation times with IFNγ (10 ng/ml), cyt-PTPε and RPTPε mRNA expression was analyzed by RT-qPCR and expressed as $2^{\Delta\Delta CT}$ over GAPDH mRNA expression (n=3–6). (B,C) Following a 24-h stimulation with IFNγ (10 ng/ml) or IL-1β (10 ng/ml), cyt-PTPε and RPTPε protein expression was analyzed by western blot densitometry and expressed as relative intensity corrected for vinculin expression. Representative western blots are shown (control lanes in B are reproduced here from Fig. 1D for comparison); dotted lines indicate where the image of the membrane has been modified to remove lanes irrelevant to the result (B, n=6; C. n=7). Data are expressed as mean±s.e.m. *$P<0.05$, **$P<0.005$, ***$P<0.001$, ****$P<0.0001$ by (A) one-way ANOVA with Tukey's multiple comparisons post-test and (B,C) Wilcoxon test.

the interval between monocyte isolation [day (D)0] and overnight incubation (D1). As shown in Fig. 4A,B, both cyt-PTPε and RPTPε mRNA and cyt-PTPε protein expression were upregulated during overnight adherence. However, when adherence was prevented by using low-binding tubes or continuous stirring, there was no increased expression of PTPε (Fig. S4). This treatment was without any significant effect on PTP-1B expression, a phosphatase used as a control.

In order to verify the link between PTPε and monocyte adhesion, we used PTPε-specific siRNAs (siPTPε). We found that siPTPε

preferentially reduced RPTPε expression in transfected monocytes (Fig. S5A) and resulted in a reduced cell adhesion when compared with control siRNA (siCTRL)-transfected cells (Fig. 4C), suggesting the involvement of RPTPε in monocyte adhesion.

PTPε is involved in migration

Since PTPε is involved in cell adhesion and its expression is regulated during hMDM polarization and adhesion processes, it was relevant to study the role of the phosphatase in LTD4-induced migration. Myeloid cell migration requires actin rearrangement as
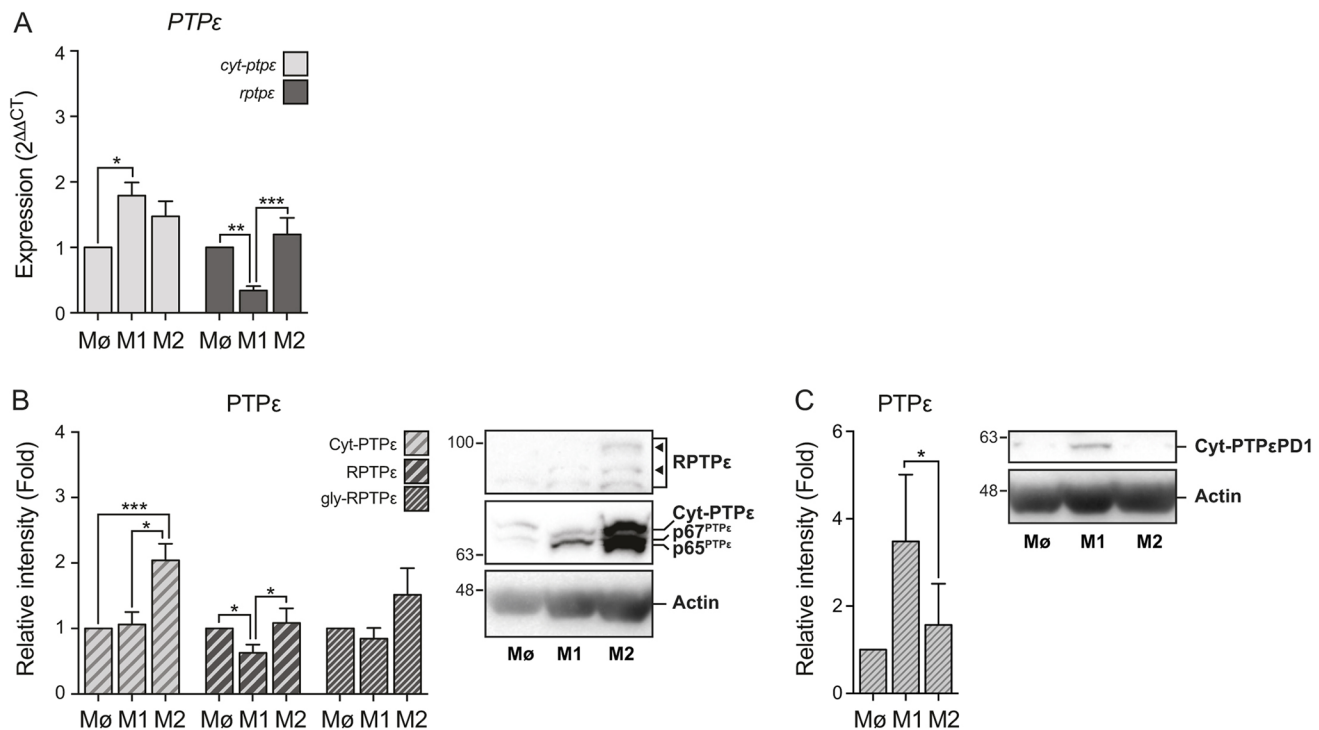
Fig. 3. Expression of multiple PTPε isoforms in hMDMs. hMDMs were differentiated and polarized, as described in the Materials and Methods section. In the resulting Mφ, and M1- and M2-polarized hMDMs, (A) cyt-PTPε and RPTPε mRNA expression was analyzed by RT-qPCR and expressed as $2^{\Delta\Delta CT}$ over RPL13A mRNA expression (n=9) and (B,C) cyt-PTPε and RPTPε protein expression was analyzed by western blot densitometry and expressed as relative intensity corrected for actin expression. A representative western blot is shown; arrowheads indicate glycosylated protein (B, n=10; C, n=10). Data are expressed as mean±s.e.m. *$P<0.05$, **$P<0.005$, ***$P<0.001$ by (A,B) one-way ANOVA with Tukey's multiple comparisons post-test or (C) Friedman with Dunn's multiple comparisons post-test.
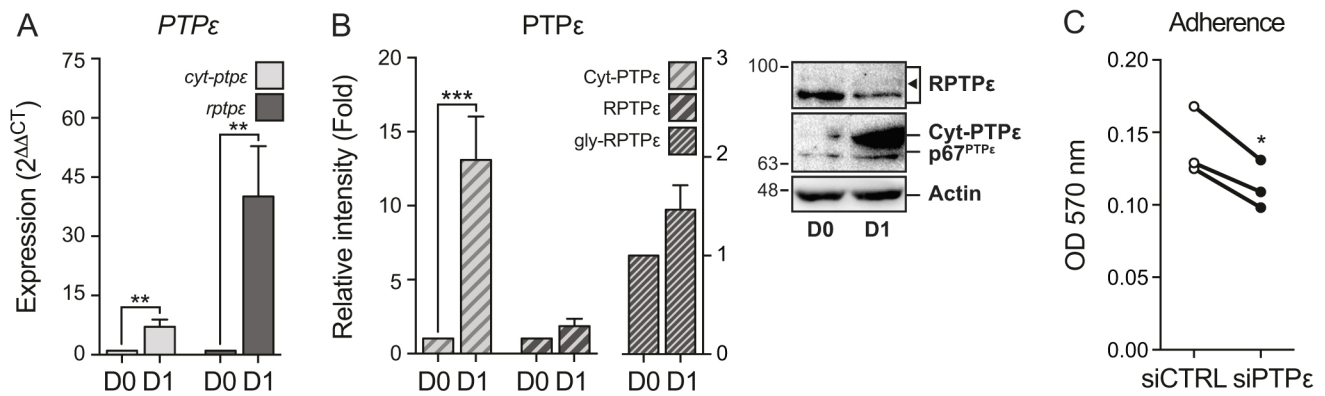
Fig. 4. RPTPε is involved in human monocyte adherence. Following their isolation from whole blood, human primary monocytes were immediately processed (D0) or left overnight in round bottom culture cell-treated polypropylene tubes (D1) for mRNA and protein expression analysis. (A) cyt-PTPε and RPTPε mRNA expression was analyzed by RT-qPCR and expressed as $2^{\Delta\Delta CT}$ over *RPL13A* mRNA expression (*n*=9). (B) cyt-PTPε and RPTPε protein expression was analyzed by western blot densitometry quantification and expressed as relative intensity corrected for actin expression. A representative western blot is shown; the arrowhead indicates glycosylated protein (*n*=10). (C) Following a 42-h transfection with siRNAs (siCTRL or siPTPε), human primary monocytes were counted and seeded for 6 h in round bottom cell culture-treated polypropylene tubes. Cells were treated as described in the Materials and Methods section for adhesion assays to quantify cell adherence (*n*=3). Data are expressed as mean±s.e.m. *$P<0.05$, **$P<0.005$, ***$P<0.001$, by (A,B) Wilcoxon test and (C) paired Student's *t*-test.

cells spread and contract throughout their movement. We used the scratch assay to compare the migration capacities of polarized hMDMs. In addition, since LTD_4 has been shown to induce actin reorganization through Rho (Saegusa et al., 2001; Massoumi et al., 2002), the ROCK inhibitor Y-27632 was used to inhibit this signaling pathway.

M2-polarized hMDMs migrated more into the scratched area, with 64.25% of the surface being filled as compared to Mφ and M1-polarized hMDMs which showed filled areas of 43.14% and 9.39%, respectively, at 24 h following the scratch (Fig. 5). Mφ hMDMs have a relatively low mobility, LTD_4 did not significantly increase their migration, whereas ROCK inhibition with Y-27632 enhanced their mobility. M1-polarized hMDMs were mostly immobile. On the other hand, while LTD_4 stimulation significantly increased M2-polarized hMDM migration, ROCK inhibition had no further impact, thus suggesting that ROCK activity could be modulated through LTD_4 stimulation in these cells. Moreover, a significant decrease in LTD_4-induced migration of siPTPε-transfected M2-polarized hMDMs was observed in a scratch assay – representing a 2D migration (Fig. 6A,B) – and 3D migration in Matrigel® Matrix (Fig. 6C,D).

PTPε is involved in podosome organization in M2-hMDMs
PTPε has been shown to regulate podosome organization in murine osteoclasts (Chiusaroli et al., 2004; Granot-Attas et al., 2009; Finkelshtein et al., 2014), cells which are derived from the same myeloid lineage as macrophages. Interestingly, it has previously been shown that M2-polarized hMDMs are the only ones to use podosomes to move via mesenchymal migration (Cougoule et al., 2012). We therefore explored the role of PTPε in podosome formation in these differentiated cells.

Following transfection with siPTPε, a different organization of podosomes was observed in M2-polarized hMDMs, when compared with siCTRL-transfection, whereas podosome organization in Mφ and M1-polarized hMDMs showed no difference (Fig. 7A). siCTRL-transfected M2-polarized hMDMs showed a homogeneous distribution of podosomes on the adherent membrane, but siPTPε-transfected M2-polarized hMDMs showed podosome clusters unevenly distributed throughout the cell and in reduced numbers. This uneven distribution was also observed following LTD_4 stimulation. However, ROCK inhibition allowed the recovery of

podosome distribution, organization and numbers in siPTPε-transfected M2-polarized hMDMs (Fig. 7B,C).

ROCK2 phosphorylation status depends on RPTPε
Following the identification of a role for PTPε in migration in M2-polarized hMDMs, we were interested in understanding the signaling pathways leading to this migration. Since Y-27632 inhibits ROCK activation and facilitates mesenchymal migration (Gui et al., 2014), the phosphorylation status of this kinase was investigated. M2-polarized hMDMs were transfected with siPTPε and stimulated with LTD_4 for 0 to 60 min. A statistically significant increase of ROCK2 Tyr-722 phosphorylation (at the inhibitory site) was seen following siPTPε transfection when compared with siCTRL (Fig. 8A), suggesting that decreased presence of PTPε results in decreased activity of ROCK2.

HEK-293 cells stably transfected with $CysLT_1R$ (HEK-LT1), allowed us to study the role of the two PTPε isoforms, independently. HEK-LT1 were transiently transfected with cyt-PTPε, RPTPε or an empty vector (pcDNA3) and stimulated with LTD_4 for 0 to 60 min. As determined by western blot densitometry, an increase in phosphorylation of the inhibitory ROCK2 Tyr-722 residue was observed with a maximum between 20 and 30 min for the control (pcDNA3) and the cyt-PTPε transfection. However, a statistically significant decrease of ROCK2 Tyr-722 phosphorylation was seen following RPTPε transfection when compared with cyt-PTPε and control (pcDNA3) (Fig. 8B).

Since only RPTPε inhibited LTD_4-induced ROCK2 Tyr-722 phosphorylation, and the majority of this isoform is glycosylated in M2-polarized hMDMs, we were interested in investigating whether glycosylation was involved in RPTPε activity. Extracellular putative N-glycosylated residues (residue 23 and 30) of RPTPε were therefore mutated from asparagine to glutamine residues (N23Q and N30Q). Each individual mutant was glycosylated at a lower level than the WT protein, indicating that both residues are glycosylated (Fig. S6B). The mutants were expressed at the same level and in the same cellular localization as the wild-type construction (WT) (Fig. S6C,D). We then examined the effect of the RPTPε mutants on LTD_4-stimulated ROCK2 Tyr-722 phosphorylation. As shown in Fig. 8C, transfection of both mutants resulted in higher ROCK2 Tyr-722 phosphorylation compared to RPTPε-WT. Thus ROCK2 was less active in the presence of the glycosylation mutants than in the presence of the WT phosphatase. Interestingly, mutation of
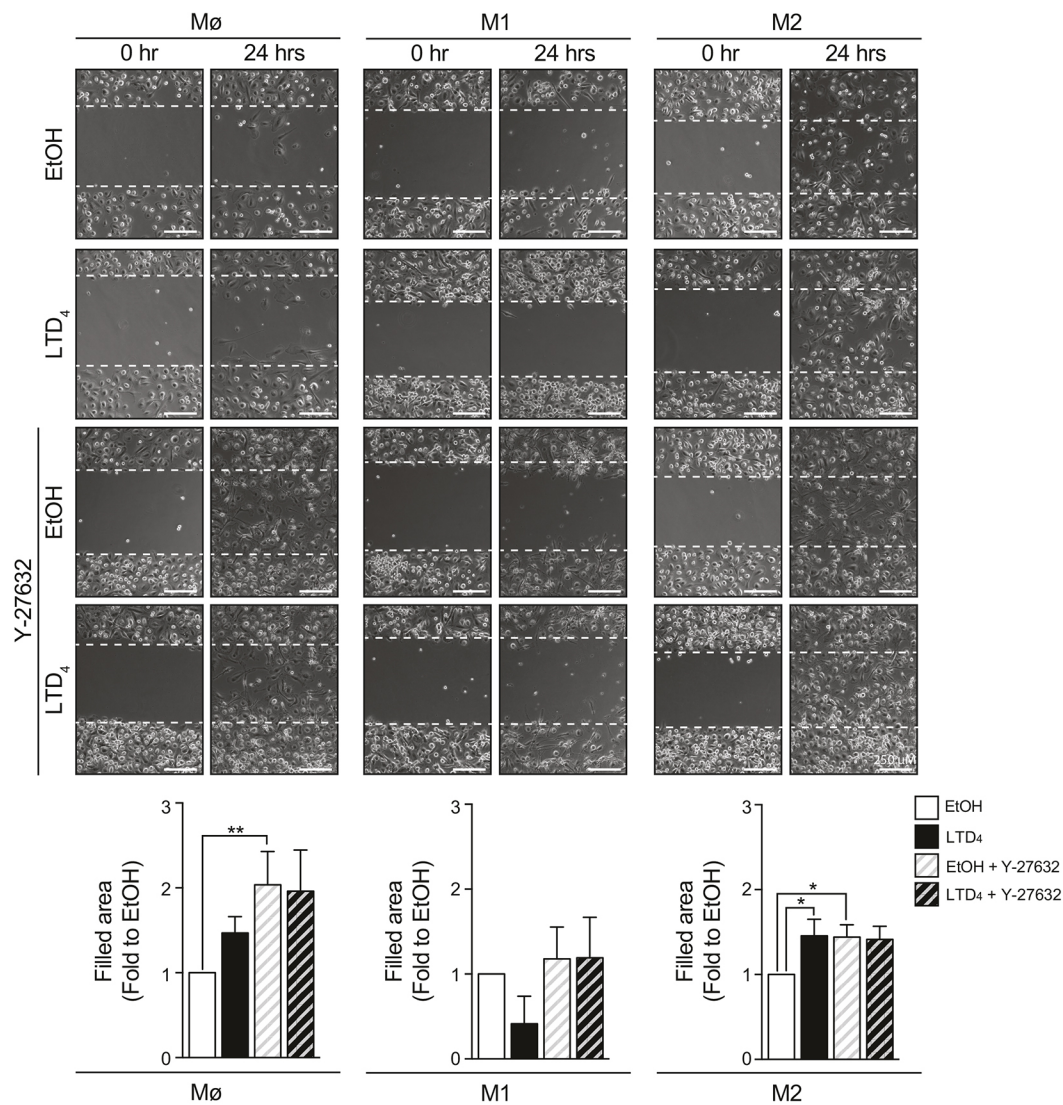
Fig. 5. M2-polarized macrophages use mesenchymal migration. hMDMs were differentiated and polarized, as described in the Materials and Methods section. Following polarization, a scratch was made in the resulting Mφ, M1- and M2-polarized hMDMs layers. Cells were incubated with LTD$_4$ (100 nM), or its vehicle (EtOH), with or without Y-27632 (20 µM) for 24 h and photographs were taken to quantify scratch closure. A representative experiment is shown while graphs, at the bottom, represent the compilation of data from all experiments (n=6). Data are expressed as mean±s.e.m. *P<0.05, **P<0.005, by Friedman test with Dunn's multiple comparisons post-test. Scale bars: 250 µm.

both residues produced a protein whose activity towards ROCK2 phosphorylation was comparable to the single mutants (results not shown). Thus, glycosylation of RPTPε has at least a partial role in its activity since the mutation of the residues N23 and N30 decreases the effect of RPTPε on the phosphorylation levels of ROCK2 Tyr-722.

DISCUSSION

One of the main mechanisms that regulate cellular processes is the reversible phosphorylation of proteins by kinases and phosphatases. Several studies have shown that PTPs could play essential roles in physiological processes (Fischer et al., 1991) and, therefore, be involved in numerous diseases (Hendriks et al., 2013). PTPε was of interest here since it is relevant in allergic asthma (Tremblay et al., 2008) and our previous results suggested that it is involved in inflammatory processes modulated by cys-LTs. In addition, whereas previously published data showed that PTPε isoforms were expressed in a non-overlapping expression patterns in murine cell types (Elson and Leder, 1995; Gil-Henn et al., 2000), we showed

that both cyt-PTPε and RPTPε were both expressed in human primary monocytes (Lapointe et al., 2019) but their targets were divergent. Thus, the expression pattern and its possible functional significance were the focus of this study.

In the present work, we show that polarizing cytokines upregulate cyt-PTPε and RPTPε expression. Interestingly, among the Th2 polarization agents tested, IL-4 was shown to upregulate PTPε expression by a cys-LT-dependent mechanism. This is consistent with our previous results where we identified PTPε as a CysLT$_1$R signaling partner and confirmed its role in LTD$_4$-induced signaling (Lapointe et al., 2019). IFNγ and IL-1β also upregulated both cyt-PTPε and RPTPε expression. IL-1β had also been shown to upregulate cyt-PTPε in U373-MG astrocytoma cells (Schumann et al., 1998) but this is the first demonstration of PTPε upregulation by the other cytokines.

In addition, expression of PTPε isoforms differs in M1- and M2-polarized hMDMs. Specifically, M2-polarized hMDMs expressed more of the highly glycosylated form of RPTPε and siPTPε-transfected
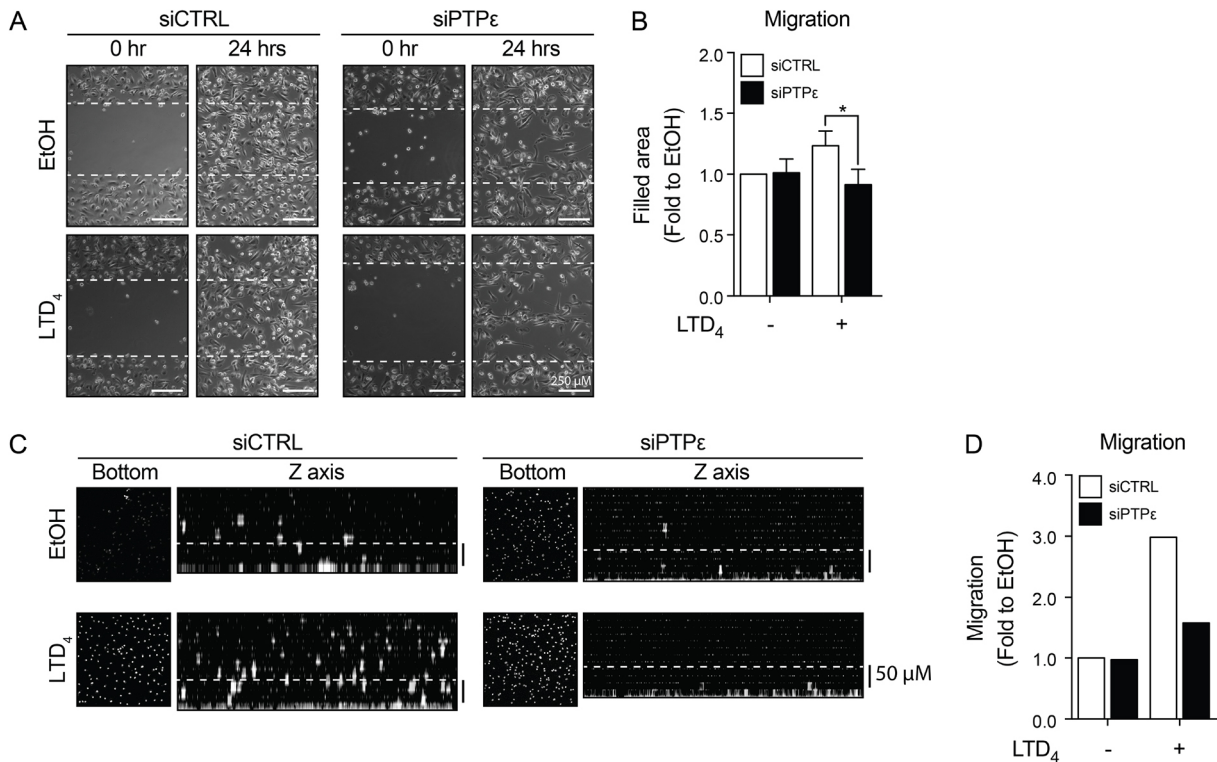
Fig. 6. RPTPε is involved in M2-polarized macrophage migration. M2-polarized hMDMs were differentiated, transfected with siRNAs (siCTRL and siPTPε), and polarized as described in the Materials and Methods section. (A,B) Following polarization, a scratch was made in the resulting siRNA-transfected M2-polarized hMDM layers. Cells were incubated with LTD$_4$ (100 nM), or its vehicle (EtOH), for 24 h and photographs were taken to quantify scratch closure. Photographs from a representative experiment are shown while graph (B) represents the compilation of all experiments (*n*=9). Data are expressed as mean ±s.e.m. *P<0.05, by two-way ANOVA with Sidak's multiple comparisons post-test. Scale bars: 250 µm. (C,D) Cells were grown in 96-well plates, and, following polarization, Matrigel® Matrix was added over the cells and migration was allowed for 48 h in the presence of LTD$_4$ (100 nM), or its vehicle (EtOH). Cell migration was quantified as described. A representative experiment is shown out of three performed. Scale bars: 50 µm.

M2-polarized hMDMs also migrated less, a possible consequence of uneven distribution of podosomes through inhibition of LTD$_4$-induced ROCK2 Tyr-722 dephosphorylation by RPTPε.

It has been shown that macrophage-like terminal differentiation of HL-60 and myeloid leukemia M1 cells increases cyt-PTPε but not RPTPε expression (Tanuma et al., 1999). We have observed that differentiation of human monocytes into macrophages upregulates RPTPε but not cyt-PTPε mRNA expression (F.L., unpublished results), indicating that both the cell type and stimulus may influence the expression of the two isotypes differentially. We therefore further examined the expression pattern of PTPε isoforms in polarized hMDMs. Interestingly, even though IL-4-stimulated monocytes only increased their expression of cyt-PTPε, M2-polarized hMDMs expressed higher levels of both RPTPε and cyt-PTPε when compared to M1-polarized hMDMs. In addition, M2-polarized hMDMs expressed more of the gly-RPTPε forms than Mφ and M1-polarized hMDMs. Moreover, monocytes, which do not usually express gly-RPTPε (Lapointe et al., 2019), increased their expression of this form following adhesion. Downregulation of RPTPε using PTPε-specific siRNA, reduced monocyte adhesion, further supporting a role for the phosphatase in the adhesion processes.

Interestingly, a role for PTPε in myeloid cell adhesion has been suggested. Murine *PTPε*$^{-/-}$ osteoclasts show defective bone adhesion and resorption as a consequence of disorganized podosomes (Granot-Attas et al., 2009; Chiusaroli et al., 2004). Our results showed that when PTPε expression was reduced in siPTPε-transfected M2-polarized hMDMs, their podosomes were decreased in numbers and found in clusters instead of being evenly distributed. Interestingly,

this was true only in M2-polarized hMDMs, whereas in Mφ or M1-polarized hMDMs the podosomes remained evenly distributed in spite of siPTPε transfection. We speculated that the higher expression of the gly-RPTPε might have a role in our findings, as this was one difference between the three subpopulations.

In murine osteoclasts, cyt-PTPε, the only isoform expressed in these cells, regulates ROCK activity through Rho signaling, leading to correct assembly, dynamics and subcellular organization of podosomes, which is crucial for efficient bone resorption (Granot-Attas et al., 2009; Chiusaroli et al., 2004). Macrophages also naturally form podosomes, but only M2-polarized hMDMs were shown to use podosomes to migrate (Cougoule et al., 2012). In our experiments, ROCK inhibition allowed a recovery of podosome distribution and organization in these cells.

In order to understand the role of RPTPε in LTD$_4$-induced ROCK phosphorylation, we studied ROCK2 Tyr-722 phosphorylation levels. Phosphorylation of Tyr-722 on ROCK2 is inhibitory, so with higher levels of phosphorylation of this residue, the kinase is inhibited. In siPTPε-transfected M2-polarized hMDMs, phosphorylation of ROCK2 Tyr-722 was increased with LTD$_4$ stimulation. Conversely, expression of RPTPε in HEK-LT1 cells resulted in the inhibition of LTD$_4$-induced ROCK2 Tyr-722 phosphorylation, potentially resulting in an activated kinase.

ROCK2 activity is regulated by various mechanisms. Of these, phosphorylation is the most studied. Phosphorylation of Ser-1366 correlates with increased kinase activity but phosphorylation of Tyr-722 has been shown to be inhibitory as it prevents RhoA-mediated ROCK2 activation (Lee et al., 2010; Lee and Chang, 2008).
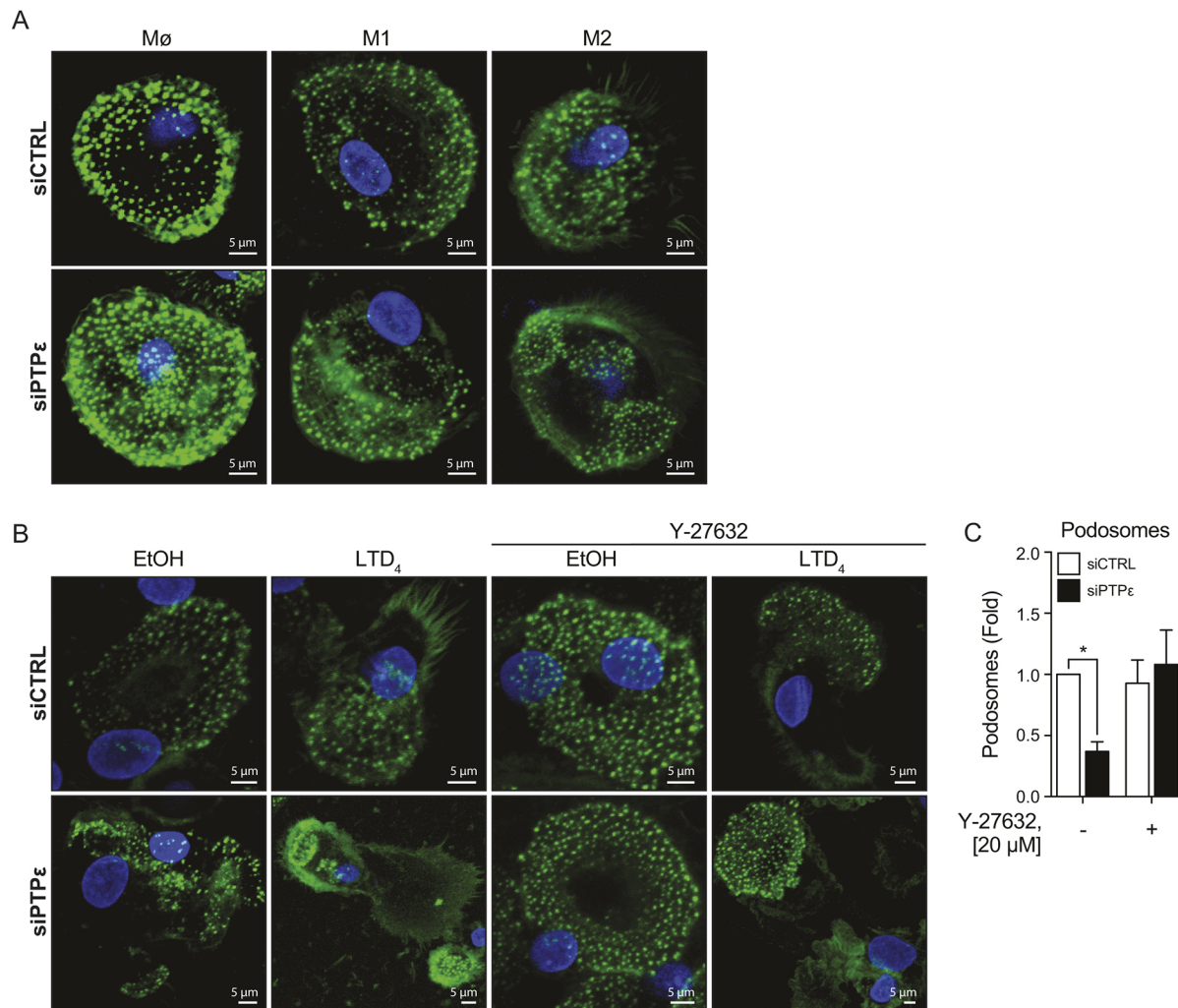
Fig. 7. RPTPε is involved in podosome organization in M2-polarized macrophages. hMDMs were differentiated, transfected with Cy™3-tagged siRNAs (siCTRL and siPTPε), and polarized as described in the Materials and Methods section. (A) Following polarization, resulting Mφ, and M1- and M2-polarized hMDMs were fixed, permeabilized, and incubated with Phalloidin–Alexa Fluor™ 488 to allow F-actin visualization, while a DAPI staining was used to visualize nuclei. (B) Following polarization, resulting M2-polarized hMDMs were stimulated with LTD$_4$, or its vehicle (EtOH), with or without Y-27632 (20 µM) for 24 h before staining as previously described. (C) Podosomes were quantified in stimulated cells from four different experiments (n=4). Data are expressed as mean±s.e.m. *P<0.05, by two-way ANOVA with Sidak's multiple comparisons post-test.
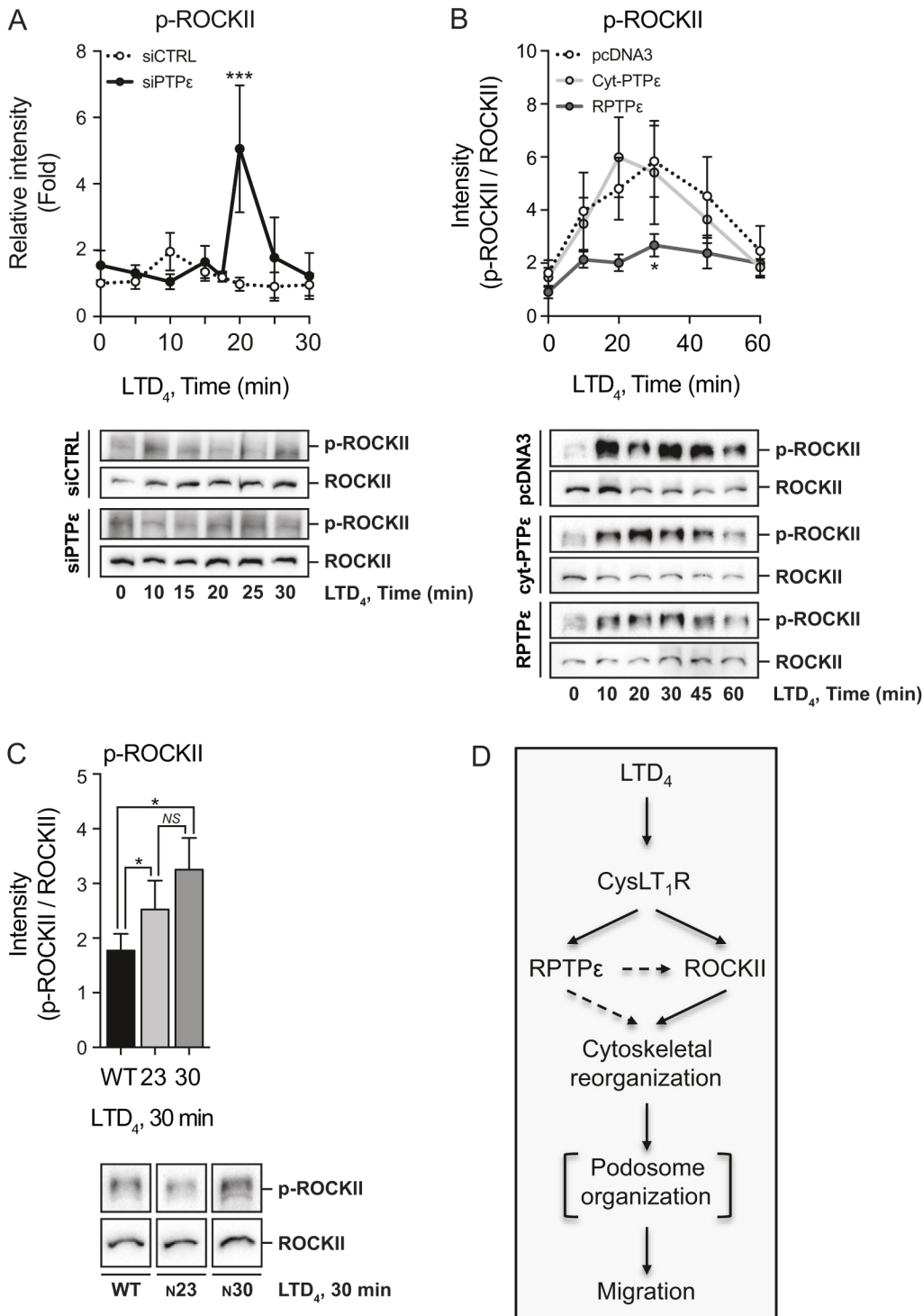
Although ROCK2 Tyr-722 phosphorylation correlates with RPTPε downregulation or overexpression, ROCK2 Tyr-722 may not be a direct substrate of RPTPε. RPTPε is known to activate Src by dephosphorylating its inhibitory Tyr-527 residue (Gil-Henn and Elson, 2003; Berman-Golan and Elson, 2007; Granot-Attas et al., 2009). Src, meanwhile, also activates SHP-2 (Salmond and Alexander, 2006), which, in turn, is a cytosolic PTP that dephosphorylates ROCK2 Tyr-722 and thus allows its activation by RhoA (Lee and Chang, 2008). By activating Src, RPTPε may therefore allow SHP-2 activation through tyrosine-phosphorylated ligand interaction and finally, SHP-2-induced ROCK2 Tyr-722 dephosphorylation. RPTPε activity would then lead to myosin light chain phosphorylation, actin contraction and podosome organization.

LTD$_4$-induced ROCK2 Tyr-722 phosphorylation was decreased with WT RPTPε expression compared to control or cyt-PTPε, but increased phosphorylation was found when either the N-glycosylated Asn-23 or Asn-30 residue was mutated to glutamine. This indicates that, at least in part, glycosylation of RPTPε is important for dephosphorylation of ROCK2 Tyr-722. However, additional PTP experiments would be necessary to establish the role of glycosylation

in RPTPε activity. We were not successful at directly examining the phosphatase activity *in vitro*, in spite of many different attempts at optimization (dissociation from magnetic beads and agarose protein G, pH modification; Hamel-Côté et al., 2019). Interestingly, RPTPα, member of the same PTP subfamily as RPTPε, only dephosphorylates the insulin receptor when glycosylated (Lammers et al., 1997). In addition, whereas the activity of RPTPε is regulated by phosphorylation in murine Neu-induced mammary tumor cells, only the glycosylated form of the phosphatase is phosphorylated at the Tyr-695 residue. The authors suggested that only the glycosylated forms of RPTPε would activate Src (Berman-Golan and Elson, 2007).

In conclusion, the present work demonstrates a unique role for RPTPε in regulating ROCK2 Tyr-722 phosphorylation (summarized in Fig. 8D) and shows that this role is enhanced through the glycosylation of the asparagine residues. Interestingly, among the myeloid cell types examined in this study, M2-polarized hMDMs expressed the glycosylated form of RPTPε, which is suggested to be involved in appropriate podosome organization through ROCK2 signaling leading to M2-polarized hMDM migration. The mutual interactions of PTPε and CysLT$_1$R signaling in inflammatory

Fig. 8. RPTPε modulates ROCK2 Tyr-722 phosphorylation.
(A) M2-polarized hMDMs were differentiated, transfected with siRNAs (siCTRL and siPTPε), and polarized as described in the Materials and Methods section. Following polarization, cells were stimulated with LTD$_4$ (100 nM), or its vehicle (EtOH), for the indicated times. Western blots were performed and densitometry analysis was used to quantify p-ROCK2 Tyr-722 expression, corrected for total ROCK2 expression. A representative western blot is shown (n=2–6). (B) HEK-LT1 cells were transiently transfected with pcDNA3, cyt-PTPε or RPTPε or (C) RPTPε-WT, RPTPε-N23Q (N23) or RPTPε-N30Q (N30), and stimulated with LTD4 (10 nM), or its vehicle (EtOH), for the indicated times. Western blots were performed and densitometry analysis was used to quantify p-ROCK2 Tyr-722 expression, corrected for total ROCK2 expression. Representative western blots are shown (B, n=4–7; C, n=3–7). Data are expressed as mean±s.e.m. *$P<0.05$, ***$P<0.001$, by (A,B) two-way ANOVA with Dunnett's multiple comparisons post-test to the control, unstimulated condition and (C) paired Student's t-test. (D) Graphic representation of how RPTPε and ROCK2 could be involved in M2-polarized macrophage migration. LTD$_4$, through CysLT$_1$R signaling leads to RPTPε activation. As a consequence, the ROCK2 inhibitory Tyr-722 is de-phosphorylated, and ROCK2 is activated, allowing ROCK2 to play its role in cytoskeletal reorganization. This reorganization leads to podosome organization and M2-polarized hMDM migration.

diseases, and especially asthma, deserve further studies since that would potentially lead to novel intervention models.

MATERIALS AND METHODS
Antibodies and reagents
Antibodies against the multiple PTPε isoforms (ab123345) and phosphorylated ROCK2 Y-722 (ab182649) were purchased from Abcam® PLC (Toronto, ON, Canada). Total ROCK2 antibodies were from Santa Cruz Biotechnologies, Inc. (sc-398519, Santa Cruz, CA). Specific antibodies against vinculin (V4505) and actin (A5060) were purchased from Sigma-Aldrich® (Oakville, ON, Canada).

Secondary antibodies conjugated to the horseradish peroxidase (HRP) (7074, 7076) used in western blot detection were from Cell Signaling Technology® (Danvers, MA). Alexa Fluor™ 488–phalloidin was from Thermo Fisher Scientific (Burlington ON, Canada) and DAPI, from Molecular Probes® (Burlington, ON, Canada).

LTD$_4$ and MK886, a 5-lipoxygenase activating protein inhibitor, were purchased from Cayman Chemical Company (Ann Arbor, MI). Y-27632 was from Sigma-Aldrich®. Matrigel® Matrix was from Corning Inc. (Tewksbury, MA, USA).

Leupeptin, aprotinin, phenylmethanesulfonyl fluoride (PMSF), pepstatin A, and the Phosphatase Inhibitor Cocktail II (PICII) were purchased from

Sigma-Aldrich®. Sodium fluoride (NaF) was from Thermo Fisher Scientific, sodium orthovanadate (Na$_3$VO$_4$), from Bio Basic Canada Inc. (Markham, ON, Canada), and Complete Mini EDTA-free protease inhibitor tablets were from Roche Diagnostics (Laval, QC, Canada).

Finally the transfection reagent used for transient transfection was TransIT®-LT1 (Mirus® Bio LLC, Madison, WI).

Plasmids
Plasmids used in this work were cyt-PTPε and RPTPε, stabilized by a 5′ β-globin intron and under the control of a CMV promoter, subcloned into a pcDNA3 vector (Invitrogen, Carlsbad, CA, USA). RPTPε was also subcloned in pGFP^2-N3(h) vector (Perkin Elmer Canada, Woodbridge, ON, Canada) in order to yield C-terminus-tagged RPTPε_GFP^2 in which asparagine residues 23 and 30 were mutated to glutamine by site-directed mutagenesis with the Q5® Site-Directed Mutagenesis Kit (New England Biolabs®, Whitby, ON, Canada) using the following primers (the mutated codon is shown in lowercase): RPTPε_N23Q forward 5′-TCTCAGGGGGC**caa**G-AGACCACTGCCGAC-3′ and RPTPε_N23Q reverse 5′-GCCCTGGC-GAGCGGCAAG-3′; RPTPε_N30Q forward 5′-TGCCGACAGC**caa**-GAGACAACCAC-3′, and RPTPε_N30Q reverse 5′-GCCCTGGCGAG-CGGCAAG-3′.

siRNAs and Cy™3-tagged siRNAs used in this study were from Ambion® (Burlington, ON, Canada; cat. number: 4390828, code ADFARDD).

Cells
HEK-293 cells (ATCC®) stably expressing CysLT$_1$R (HEK-LT1), as described in Thompson et al. (2006), were cultured in Dulbecco's modified Eagle's medium (DMEM) (Gibco®, Burlington, ON, Canada), supplemented with 5% fetal bovine serum (FBS) (PAA, Piscataway, NJ). Experiments were performed 48 h post-transfection of these cells. HEK-LT1 cells are regularly controlled for their expression of CysLT1R and tested for mycoplasma contamination.

Human primary monocytes were isolated from peripheral blood mononuclear leukocytes obtained from healthy donors after informed written consent, in accordance with a Université de Sherbrooke Human Ethics Review Board-approved protocol (#2016-1167-CysLT), adhering to the Helsinki agreement. Cells were processed as previously described (Lapointe et al., 2019). Isolated monocytes were suspended in RPMI 1640 medium (Gibco®) supplemented with 5% FBS. Experiments were performed after an overnight incubation following their isolation or 48 h post-transfection.

hMDMs were differentiated in 12- or 96-well non-treated culture plates at 5×10^5 cells/ml or on pre-treated poly-L-lysine (0.1 mg/ml) (Sigma-Aldrich®) coverslips at 1.25×10^5 cells/ml and obtained following 8 days of differentiation in RPMI 1640 medium containing 10% FBS and 20 ng/ml M-CSF (recombinant human M-CSF from E. coli: PeproTech Canada, Montreal, QC, Canada; 300-25). On day 7, medium was replaced with fresh RPMI plus 5% FBS. M1 and M2 macrophages were obtained following a 18 h polarization using, respectively, 100 ng/ml lipopolysaccharide (LPS from E. coli O127: B8, Sigma-Aldrich®; L-3129) plus 10 ng/ml IFNγ (recombinant human IFNγ from E.coli: PeproTech Canada; 300-02) or 20 ng/ml IL-4 (recombinant human IL-4 from E. coli: PeproTech Canada; 200-04).

Cells were incubated under normal conditions in a humidified atmosphere with 5% CO$_2$ at 37°C.

Adhesion assays
Following their isolation, 4×10^6 human primary monocytes were transfected with 150 pmole siRNAs for 42 h. Cells were then counted and seeded in a round-bottom polypropylene tube. Following a 6-h incubation, non-adherent cells were washed twice with PBS and resting adherent cells were fixed with 2% paraformaldehyde and stained with Crystal Violet (0.05% Crystal Violet, Sigma-Aldrich®, 25% EtOH). Cells were washed with water until no more dye was present. A 1% SDS solution was added to the tubes to solubilize the stain and tubes were agitated on orbital shaker until color was uniform. Supernatants were transferred in a 96-well plate and absorbance was read at 570 nm.

Scratch assays
hMDM migration activity was assessed with scratch assays. Following an 18-h polarization time, the cell monolayer was scratched with a sterile 10 µl micropipette tip. The scratches were immediately imaged for the zero-time point using a Leica DM-IRBE inverted microscope. Cells were subsequently incubated with Y-27632 (20 µM) for 15 min followed by a 24-h incubation with 100 nM LTD$_4$ or its vehicle (EtOH). Photographs were taken following the 24 h stimulating time. The images were used to measure the scratched area at zero-time point (T$_0$) and 24 h following the scratches (T$_{24}$), using a macro (Montpellier RIO Imaging) for ImageJ. For each condition, five photographs were taken per well and the means were used in the formula ((T$_0$−T$_{24}$)/T$_0$)×100 to calculate the percentage of the scratch closure. Filled areas are either expressed as percentage of initial or as fold change compared to EtOH.

Three-dimensional migration assays
hMDM three-dimensional migration activity was assessed in Matrigel® Matrix. hMDMs were differentiated in 96-well plates, transfected with siRNAs (siCTRL or siPTPε), and polarized to M2 as previously described. Following polarization, culture medium was removed and 50 µl Matrigel® Matrix was added directly over the cells. The matrix was allowed to polymerize for 30 min and was rehydrated for 2 h with RPMI plus 5% de-complemented autologous serum at 37°C plus 5% CO$_2$. For the migration assay, hydration medium was removed and 25 µl of 0.3% agar containing LTD$_4$ (100 nM), or its vehicle (EtOH), were added over the matrix. Cell migration was then allowed at 37°C plus 5% CO$_2$ for 48 h. Cells were then fixed in the matrix with 0.5% paraformaldehyde, permeabilized with 0.1% Triton and a DAPI staining was used to visualize nuclei. Quantification of cell migration was performed using an Olympus FluoView FV1000 confocal microscope (Center Valley, PA). Photographs were taken with a 10× objective at constant 25 µm intervals from the bottom of the wells to the top of the matrix. Nuclei were counted with Image-Pro Plus 6.0 from MediaCybernetics (Bethesda, MD). The percentage of migration was obtained as the ratio of cells counted in the first 50 µm within the matrix of the total number of cells.

Laser scanning confocal microscopy for podosome imaging
Cells were differentiated on pre-treated poly-L-lysine (0.1 mg/ml) coverslips. Adherent cells were fixed with 2% paraformaldehyde and permeabilized with 0.1% saponin. A 2% BSA solution was used to block non-specific sites. Alexa Fluor™ 488–phalloidin (1:500) was used to visualize F-actin and DAPI staining (1:1000) was used to visualize nuclei. Finally, cells transfected with the Cy™3-tagged siRNAs were visualized and analyzed using an Olympus FluoView FV1000 confocal microscope. Captured images were further analyzed using Image-Pro Plus 6.0 from MediaCybernetics.

RNA isolation and RT-PCR
Total RNA was purified using Trizol® Reagent (Thermo Fisher Scientific) according to the manufacturer's instructions using the conventional phenol/chloroform technique. To exclude genomic DNA contamination, RNA was digested with gDNA Wipeout, provided in the QuantiTect® Reverse Transcription Kit (Qiagen Inc.). First-strand cDNA synthesis was performed on 1 µg RNA using random primers supplied in the above-mentioned kit.

Real-time quantitative PCR
RT-qPCR was performed using the Rotor Gene RG-3000 from Corbett Research (San Francisco, CA, USA) as previously described (Lapointe et al., 2019). Data analysis was performed according to the 2^{ΔΔCT} method (Dussault and Pouliot, 2006). The primer sequences were as follows: RPL13A forward 5′-GTGCGTCTGAAGCCTACAAG-3′, RPL13A reverse 5′-TCTTCTCCACGTTCTTCTCG-3′, GAPDH forward 5′-TCAACGGA TTTGGTCGTATTGG-3′, GAPDH reverse 5′-GATGGGATTTCCATTGA TGACA-3′, cyt-PTPε forward 5′-CTTTTCCCGGCTCACCTGGTTC-3′, cyt-PTPε reverse 5′-GGATGGGAAAATACTTCTTGG-3′, RPTPε forward 5′-GCCTACTTCTTCAGGTTCAGG-3′, RPTPε reverse 5′-G-GATGGGAAAATACTTCTTGG-3′.

Cyt-PTPε and *RPTPε* mRNA expression were analyzed by RT-qPCR and expressed as 2^{ΔΔCT} over *GAPDH* mRNA expression in human primary monocytes. However, *RPL13A* mRNA was used as a housekeeping control when studying mRNA expression in hMDMs since its expression was more

stable between the multiple differentiation and polarization states when compared to *GAPDH*.

Western blotting

Western blotting was performed as previously described (Lapointe et al., 2019). HEK-LT1 cells were lysed using buffer containing 1% NP-40 (20 mM Tris-HCl pH 8.0, 137 mM NaCl, 1% NP-40 and 10% glycerol) and containing the inhibitors 1 mM PMSF, 2 µg/ml aprotinin, 10 µg/ml leupeptin, 1 µg/ml pepstatin A, 10 mM NaF, 1 mM Na_3VO_4, PICII 1× and a Complete Mini EDTA free protease inhibitor tablet, for 30 min on ice. Total protein concentrations were quantified using Pierce™ Coomassie Plus Assay Kit (Thermo Fisher Scientific™) and 30 µg were separated on a 10% SDS-PAGE and transferred onto a 0.45 µM nitrocellulose membrane (GE Healthcare Life Sciences). The membrane was incubated with the primary antibodies(PTPε, 1:1000; vinculin, 1:2500; actin, 1:2500; p-ROCK2, 1:1000) overnight at 4°C in 1× TBS with 0.05% Tween-20 and 5% BSA for phosphorylated proteins or a 1× TBS with 0.05% Tween-20 and 5% free-fat milk solution for non-phosphorylated proteins. Proteins were detected after to a 30-min incubation with secondary antibodies labeled with HRP (anti-mouse-Ig, 1:2500) (anti-rabbit-Ig, 1:2500) using an ECL detection system (GE Healthcare Life Sciences) on a ChemiDoc™ MP Imaging System (Bio-Rad, Mississauga, ON, Canada). Signal intensity was quantified by densitometry using Image Lab. Following phosphorylated protein detection, membranes were stained for total ROCK2 protein (ROCK2, 1:1000) after a 20-min stripping protocol (200 mM glycine, 3.5 mM SDS, 1% Tween-20 pH 2.2).

Statistical analysis

One and two-way ANOVA and Student's *t*-test (two-tailed) analyses with correction for multiple comparisons using statistical hypothesis testing were performed when required using Prism 7.0 software (GraphPad). A *P* value of <0.05 was considered statistically significant.

Supplementary information
Supplementary information available online at
http://jcs.biologists.org/lookup/doi/10.1242/jcs.234641.supplemental

References
Amano, M., Ito, M., Kimura, K., Fukata, Y., Chihara, K., Nakano, T., Matsuura, Y. and Kaibuchi, K. (1996). Phosphorylation and activation of myosin by Rho-associated kinase (Rho-kinase). *J. Biol. Chem.* **271**, 20246-20249. doi:10.1074/jbc.271.34.20246

Amano, M., Chihara, K., Kimura, K., Fukata, Y., Nakamura, N., Matsuura, Y. and Kaibuchi, K. (1997). Formation of actin stress fibers and focal adhesions enhanced by Rho-kinase. *Science* **275**, 1308-1311. doi:10.1126/science.275.5304.1308

Amano, M., Chihara, K., Nakamura, N., Kaneko, T., Matsuura, Y. and Kaibuchi, K. (1999). The COOH terminus of Rho-kinase negatively regulates rho-kinase activity. *J. Biol. Chem.* **274**, 32418-32424. doi:10.1074/jbc.274.45.32418

Amano, M., Nakayama, M. and Kaibuchi, K. (2010). Rho-kinase/ROCK: A key regulator of the cytoskeleton and cell polarity. *Cytoskeleton* **67**, 545-554. doi:10.1002/cm.20472

Berman-Golan, D. and Elson, A. (2007). Neu-mediated phosphorylation of protein tyrosine phosphatase epsilon is critical for activation of Src in mammary tumor cells. *Oncogene* **26**, 7028-7037. doi:10.1038/sj.onc.1210505

Bhuwania, R., Cornfine, S., Fang, Z., Kruger, M., Luna, E. J. and Linder, S. (2012). Supervillin couples myosin-dependent contractility to podosomes and enables their turnover. *J. Cell Sci.* **125**, 2300-2314. doi:10.1242/jcs.100032

Calle, Y., Carragher, N. O., Thrasher, A. J. and Jones, G. E. (2006). Inhibition of calpain stabilises podosomes and impairs dendritic cell motility. *J. Cell Sci.* **119**, 2375-2385. doi:10.1242/jcs.02939

Carman, C. V., Sage, P. T., Sciuto, T. E., De La Fuente, M. A., Geha, R. S., Ochs, H. D., Dvorak, H. F., Dvorak, A. M. and Springer, T. A. (2007). Transcellular diapedesis is initiated by invasive podosomes. *Immunity* **26**, 784-797. doi:10.1016/j.immuni.2007.04.015

Chiusaroli, R., Knobler, H., Luxenburg, C., Sanjay, A., Granot-Attas, S., Tiran, Z., Miyazaki, T., Harmelin, A., Baron, R. and Elson, A. (2004). Tyrosine phosphatase epsilon is a positive regulator of osteoclast function in vitro and in vivo. *Mol. Biol. Cell* **15**, 234-244. doi:10.1091/mbc.e03-04-0207

Chuang, H.-H., Yang, C.-H., Tsay, Y.-G., Hsu, C.-Y., Tseng, L.-M., Chang, Z.-F. and Lee, H.-H. (2012). ROCKII Ser1366 phosphorylation reflects the activation status. *Biochem. J.* **443**, 145-151. doi:10.1042/BJ20111839

Chuang, H.-H., Liang, S.-W., Chang, Z.-F. and Lee, H.-H. (2013). Ser1333 phosphorylation indicates ROCKI activation. *J. Biomed. Sci.* **20**, 83. doi:10.1186/1423-0127-20-83

Collin, O., Na, S., Chowdhury, F., Hong, M., Shin, M. E., Wang, F. and Wang, N. (2008). Self-organized podosomes are dynamic mechanosensors. *Curr. Biol.* **18**, 1288-1294. doi:10.1016/j.cub.2008.07.046

Cougoule, C., Van Goethem, E., Le Cabec, V., Lafouresse, F., Dupré, L., Mehraj, V., Mège, J.-L., Lastrucci, C. and Maridonneau-Parini, I. (2012). Blood leukocytes and macrophages of various phenotypes have distinct abilities to form podosomes and to migrate in 3D environments. *Eur. J. Cell Biol.* **91**, 938-949. doi:10.1016/j.ejcb.2012.07.002

Doran, J. D., Liu, X., Taslimi, P., Saadat, A. and Fox, T. (2004). New insights into the structure-function relationships of Rho-associated kinase: a thermodynamic and hydrodynamic study of the dimer-to-monomer transition and its kinetic implications. *Biochem. J.* **384**, 255-262. doi:10.1042/BJ20040344

Draijer, C., Robbe, P., Boorsma, C. E., Hylkema, M. N. and Melgert, B. N. (2013). Characterization of macrophage phenotypes in three murine models of house-dust-mite-induced asthma. *Mediators Inflamm.* **2013**, 632049. doi:10.1155/2013/632049

Draijer, C., Boorsma, C. E., Robbe, P., Timens, W., Hylkema, M. N., Ten Hacken, N. H., Van Den Berge, M., Postma, D. S. and Melgert, B. N. (2017). Human asthma is characterized by more IRF5+ M1 and CD206+ M2 macrophages and less IL-10+ M2-like macrophages around airways compared with healthy airways. *J. Allergy Clin. Immunol.* **140**, 280-283.e3. doi:10.1016/j.jaci.2016.11.020

Dussault, A.-A. and Pouliot, M. (2006). Rapid and simple comparison of messenger RNA levels using real-time PCR. *Biol. Proced. Online* **8**, 1-10. doi:10.1251/bpo114

Elson, A. and Leder, P. (1995). Identification of a cytoplasmic, phorbol ester-inducible isoform of protein tyrosine phosphatase epsilon. *Proc. Natl. Acad. Sci. USA* **92**, 12235-12239. doi:10.1073/pnas.92.26.12235

Evans, J. G., Correia, I., Krasavina, O., Watson, N. and Matsudaira, P. (2003). Macrophage podosomes assemble at the leading lamella by growth and fragmentation. *J. Cell Biol.* **161**, 697-705. doi:10.1083/jcb.200212037

Feng, J., Ito, M., Kureishi, Y., Ichikawa, K., Amano, M., Isaka, N., Okawa, K., Iwamatsu, A., Kaibuchi, K., Hartshorne, D. J. et al. (1999). Rho-associated kinase of chicken gizzard smooth muscle. *J. Biol. Chem.* **274**, 3744-3752. doi:10.1074/jbc.274.6.3744

Finkelshtein, E., Lotinun, S., Levy-Apter, E., Arman, E., Den Hertog, J., Baron, R. and Elson, A. (2014). Protein tyrosine phosphatases epsilon and alpha perform nonredundant roles in osteoclasts. *Mol. Biol. Cell* **25**, 1808-1818. doi:10.1091/mbc.e14-03-0788

Fischer, E. H., Charbonneau, H. and Tonks, N. K. (1991). Protein tyrosine phosphatases: a diverse family of intracellular and transmembrane enzymes. *Science* **253**, 401-406. doi:10.1126/science.1650499

Gant, V., Cluzel, M., Shakoor, Z., Rees, P. J., Lee, T. H. and Hamblin, A. S. (1992). Alveolar macrophage accessory cell function in bronchial asthma. *Am. Rev. Respir Dis* **146**, 900-904. doi:10.1164/ajrccm/146.4.900

Gerhardt, T. and Ley, K. (2015). Monocyte trafficking across the vessel wall. *Cardiovasc. Res.* **107**, 321-330. doi:10.1093/cvr/cvv147

Gil-Henn, H. and Elson, A. (2003). Tyrosine phosphatase-epsilon activates Src and supports the transformed phenotype of Neu-induced mammary tumor cells. *J. Biol. Chem.* **278**, 15579-15586. doi:10.1074/jbc.M210273200

Gil-Henn, H., Volohonsky, G., Toledano-Katchalski, H., Gandre, S. and Elson, A. (2000). Generation of novel cytoplasmic forms of protein tyrosine phosphatase epsilon by proteolytic processing and translational control. *Oncogene* **19**, 4375-4384. doi:10.1038/sj.onc.1203790

Gil-Henn, H., Volohonsky, G. and Elson, A. (2001). Regulation of protein-tyrosine phosphatases alpha and epsilon by calpain-mediated proteolytic cleavage. *J. Biol. Chem.* **276**, 31772-31779. doi:10.1074/jbc.M103395200

Girodet, P.-O., Nguyen, D., Mancini, J. D., Hundal, M., Zhou, X., Israel, E. and Cernadas, M. (2016). Alternative macrophage activation is increased in asthma. *Am. J. Respir. Cell Mol. Biol.* 55, 467-475. doi:10.1165/rcmb.2015-0295OC

Granot-Attas, S., Luxenburg, C., Finkelshtein, E. and Elson, A. (2009). Protein tyrosine phosphatase epsilon regulates integrin-mediated podosome stability in osteoclasts by activating Src. *Mol. Biol. Cell* 20, 4324-4334. doi:10.1091/mbc.e08-11-1158

Gui, P., Labrousse, A., Van Goethem, E., Besson, A., Maridonneau-Parini, I. and Le Cabec, V. (2014). Rho/ROCK pathway inhibition by the CDK inhibitor p27(kip1) participates in the onset of macrophage 3D-mesenchymal migration. *J. Cell Sci.* 127, 4009-4023. doi:10.1242/jcs.150987

Guiet, R., Van Goethem, E., Cougoule, C., Balor, S., Valette, A., Al Saati, T., Lowell, C. A., Le Cabec, V. and Maridonneau-Parini, I. (2011). The process of macrophage migration promotes matrix metalloproteinase-independent invasion by tumor cells. *J. Immunol.* 187, 3806-3814. doi:10.4049/jimmunol.1101245

Hamel-Côté, G., Lapointe, F. and Stankova, J. (2019). Measuring GPCR-induced activation of protein tyrosine phosphatases (PTP) using in-gel and colorimetric PTP assays. *Methods Mol. Biol.* 1947, 241-256. doi:10.1007/978-1-4939-9121-1_13

Hay, D. W. P., Torphy, T. J. and Undem, B. J. (1995). Cysteinyl leukotrienes in asthma: old mediators up to new tricks. *Trends Pharmacol. Sci.* 16, 304-309. doi:10.1016/S0165-6147(00)89059-8

Hendriks, W. J. A. J., Elson, A., Harroch, S., Pulido, R., Stoker, A. and Den Hertog, J. (2013). Protein tyrosine phosphatases in health and disease. *FEBS J.* 280, 708-730. doi:10.1111/febs.12000

Hsieh, F. H., Lam, B. K., Penrose, J. F., Austen, K. F. and Boyce, J. A. (2001). T helper cell type 2 cytokines coordinately regulate immunoglobulin E-dependent cysteinyl leukotriene production by human cord blood-derived mast cells: profound induction of leukotriene C(4) synthase expression by interleukin 4. *J. Exp. Med.* 193, 123-133. doi:10.1084/jem.193.1.123

Jenkins, S. J., Ruckerl, D., Cook, P. C., Jones, L. H., Finkelman, F. D., Van Rooijen, N., Macdonald, A. S. and Allen, J. E. (2011). Local macrophage proliferation, rather than recruitment from the blood, is a signature of TH2 inflammation. *Science* 332, 1284-1288. doi:10.1126/science.1204351

Kawano, Y., Fukata, Y., Oshiro, N., Amano, M., Nakamura, T., Ito, M., Matsumura, F., Inagaki, M. and Kaibuchi, K. (1999). Phosphorylation of myosin-binding subunit (MBS) of myosin phosphatase by Rho-kinase in vivo. *J. Cell Biol.* 147, 1023-1038. doi:10.1083/jcb.147.5.1023

Kuo, S.-L., Chen, C.-L., Pan, Y.-R., Chiu, W.-T. and Chen, H.-C. (2018). Biogenesis of podosome rosettes through fission. *Sci. Rep.* 8, 524. doi:10.1038/s41598-017-18861-2

Lammers, R., Møller, N. P. H. and Ullrich, A. (1997). The transmembrane protein tyrosine phosphatase alpha dephosphorylates the insulin receptor in intact cells. *FEBS Lett.* 404, 37-40. doi:10.1016/S0014-5793(97)00080-X

Landsman, L. and Jung, S. (2007). Lung macrophages serve as obligatory intermediate between blood monocytes and alveolar macrophages. *J. Immunol.* 179, 3488-3494. doi:10.4049/jimmunol.179.6.3488

Lapointe, F., Turcotte, S., Veronneau, S., Rola-Pleszczynski, M. and Stankova, J. (2019). Role of protein tyrosine phosphatase epsilon (PTPε) in LTD4-induced CXCL8 Expression. *J. Pharmacol. Exp. Ther.* 369, 270-281. doi:10.1124/jpet.118.255422

Lee, H.-H. and Chang, Z.-F. (2008). Regulation of RhoA-dependent ROCKII activation by Shp2. *J. Cell Biol.* 181, 999-1012. doi:10.1083/jcb.200710187

Lee, H.-H., Tien, S.-C., Jou, T.-S., Chang, Y.-C., Jhong, J.-G. and Chang, Z.-F. (2010). Src-dependent phosphorylation of ROCK participates in regulation of focal adhesion dynamics. *J. Cell Sci.* 123, 3368-3377. doi:10.1242/jcs.071555

Lee, Y. G., Jeong, J. J., Nyenhuis, S., Berdyshev, E., Chung, S., Ranjan, R., Karpurapu, M., Deng, J., Qian, F., Kelly, E. A. B. et al. (2015). Recruited alveolar macrophages, in response to airway epithelial-derived monocyte chemoattractant protein 1/CCl2, regulate airway inflammation and remodeling in allergic asthma. *Am. J. Respir. Cell Mol. Biol.* 52, 772-784. doi:10.1165/rcmb.2014-0255OC

Linder, S. (2007). The matrix corroded: podosomes and invadopodia in extracellular matrix degradation. *Trends Cell Biol.* 17, 107-117. doi:10.1016/j.tcb.2007.01.002

Lowery, D. M., Clauser, K. R., Hjerrild, M., Lim, D., Alexander, J., Kishi, K., Ong, S.-E., Gammeltoft, S., Carr, S. A. and Yaffe, M. B. (2007). Proteomic screen defines the Polo-box domain interactome and identifies Rock2 as a Plk1 substrate. *EMBO J.* 26, 2262-2273. doi:10.1038/sj.emboj.7601683

Luxenburg, C., Geblinger, D., Klein, E., Anderson, K., Hanein, D., Geiger, B. and Addadi, L. (2007). The architecture of the adhesive apparatus of cultured osteoclasts: from podosome formation to sealing zone assembly. *PLoS ONE* 2, e179. doi:10.1371/journal.pone.0000179

Lynch, K. R., O'neill, G. P., Liu, Q., Im, D.-S., Sawyer, N., Metters, K. M., Coulombe, N., Abramovitz, M., Figueroa, D. J., Zeng, Z. et al. (1999). Characterization of the human cysteinyl leukotriene CysLT1 receptor. *Nature* 399, 789-793. doi:10.1038/21658

Martinez, F. O., Gordon, S., Locati, M. and Mantovani, A. (2006). Transcriptional profiling of the human monocyte-to-macrophage differentiation and polarization: new molecules and patterns of gene expression. *J. Immunol.* 177, 7303-7311. doi:10.4049/jimmunol.177.10.7303

Massoumi, R., Larsson, C. and Sjolander, A. (2002). Leukotriene D(4) induces stress-fibre formation in intestinal epithelial cells via activation of RhoA and PKCdelta. *J. Cell Sci.* 115, 3509-3515.

Matsui, T., Amano, M., Yamamoto, T., Chihara, K., Nakafuku, M., Ito, M., Nakano, T., Okawa, K., Iwamatsu, A. and Kaibuchi, K. (1996). Rho-associated kinase, a novel serine/threonine kinase, as a putative target for small GTP binding protein Rho. *EMBO J.* 15, 2208-2216. doi:10.1002/j.1460-2075.1996.tb00574.x

Mayernik, D. G., Ul-Haq, A. and Rinehart, J. J. (1983). Differentiation-associated alteration in human monocyte-macrophage accessory cell function. *J. Immunol.* 130, 2156-2160.

Murray, P. J., Allen, J. E., Biswas, S. K., Fisher, E. A., Gilroy, D. W., Goerdt, S., Gordon, S., Hamilton, J. A., Ivashkiv, L. B., Lawrence, T. et al. (2014). Macrophage activation and polarization: nomenclature and experimental guidelines. *Immunity* 41, 14-20. doi:10.1016/j.immuni.2014.06.008

Pan, Y.-R., Chen, C.-L. and Chen, H.-C. (2011). FAK is required for the assembly of podosome rosettes. *J. Cell Biol.* 195, 113-129. doi:10.1083/jcb.201103016

Pan, Y.-R., Cho, K.-H., Lee, H.-H., Chang, Z.-F. and Chen, H.-C. (2013). Protein tyrosine phosphatase SHP2 suppresses podosome rosette formation in Src-transformed fibroblasts. *J. Cell Sci.* 126, 657-666. doi:10.1242/jcs.116624

Panzer, L., Trübe, L., Klose, M., Joosten, B., Slotman, J., Cambi, A. and Linder, S. (2016). The formins FHOD1 and INF2 regulate inter- and intra-structural contractility of podosomes. *J. Cell Sci.* 129, 298-313. doi:10.1242/jcs.177691

Saegusa, S., Tsubone, H. and Kuwahara, M. (2001). Leukotriene D(4)-induced Rho-mediated actin reorganization in human bronchial smooth muscle cells. *Eur. J. Pharmacol.* 413, 163-171. doi:10.1016/S0014-2999(01)00773-7

Salmond, R. J. and Alexander, D. R. (2006). SHP2 forecast for the immune system: fog gradually clearing. *Trends Immunol.* 27, 154-160. doi:10.1016/j.it.2006.01.007

Schultze, J. L., Schmieder, A. and Goerdt, S. (2015). Macrophage activation in human diseases. *Semin. Immunol.* 27, 249-256. doi:10.1016/j.smim.2015.07.003

Schumann, G., Fiebich, B. L., Menzel, D., Hüll, M., Butcher, R., Nielsen, P. and Bauer, J. (1998). Cytokine-induced transcription of protein-tyrosine-phosphatases in human astrocytoma cells. *Brain Res. Mol. Brain Res.* 62, 56-64. doi:10.1016/S0169-328X(98)00237-X

Scott, J. P. and Peters-Golden, M. (2013). Antileukotriene agents for the treatment of lung disease. *Am. J. Respir. Crit. Care. Med.* 188, 538-544. doi:10.1164/rccm.201301-0023PP

Sebbagh, M., Renvoizé, C., Hamelin, J., Riché, N., Bertoglio, J. and Bréard, J. (2001). Caspase-3-mediated cleavage of ROCK I induces MLC phosphorylation and apoptotic membrane blebbing. *Nat. Cell Biol.* 3, 346-352. doi:10.1038/35070019

Sebbagh, M., Hamelin, J., Bertoglio, J., Solary, E. and Bréard, J. (2005). Direct cleavage of ROCK II by granzyme B induces target cell membrane blebbing in a caspase-independent manner. *J. Exp. Med.* 201, 465-471. doi:10.1084/jem.20031877

Tanuma, N., Nakamura, K. and Kikuchi, K. (1999). Distinct promoters control transmembrane and cytosolic protein tyrosine phosphatase epsilon expression during macrophage differentiation. *Eur. J. Biochem.* 259, 46-54. doi:10.1046/j.1432-1327.1999.00004.x

Thivierge, M., Staňková, J. and Rola-Pleszczynski, M. (2001). IL-13 and IL-4 up-regulate cysteinyl leukotriene 1 receptor expression in human monocytes and macrophages. *J. Immunol.* 167, 2855-2860. doi:10.4049/jimmunol.167.5.2855

Thivierge, M., Stankova, J. and Rola-Pleszczynski, M. (2006). Toll-like receptor agonists differentially regulate cysteinyl-leukotriene receptor 1 expression and function in human dendritic cells. *J. Allergy Clin. Immunol.* 117, 1155-1162. doi:10.1016/j.jaci.2005.12.1342

Thivierge, M., Stankova, J. and Rola-Pleszczynski, M. (2009). Cysteinyl-leukotriene receptor type 1 expression and function is down-regulated during monocyte-derived dendritic cell maturation with zymosan: involvement of IL-10 and prostaglandins. *J. Immunol.* 183, 6778-6787. doi:10.4049/jimmunol.0901800

Thomas, E., Ramberg, R., Sale, G., Sparkes, R. and Golde, D. (1976). Direct evidence for a bone marrow origin of the alveolar macrophage in man. *Science* 192, 1016-1018. doi:10.1126/science.775638

Thompson, C., Cloutier, A., Bossé, Y., Thivierge, M., Gouill, C. L., Larivée, P., Mcdonald, P. P., Stankova, J. and Rola-Pleszczynski, M. (2006). CysLT1 receptor engagement induces activator protein-1- and NF-kappaB-dependent IL-8 expression. *Am. J. Respir. Cell Mol. Biol.* 35, 697-704. doi:10.1165/rcmb.2005-0407OC

Toews, G. B., Vial, W. C., Dunn, M. M., Guzzetta, P., Nunez, G., Stastny, P. and Lipscomb, M. F. (1984). The accessory cell function of human alveolar macrophages in specific T cell proliferation. *J. Immunol.* 132, 181-186.

Tremblay, K., Lemire, M., Potvin, C., Tremblay, A., Hunninghake, G. M., Raby, B. A., Hudson, T. J., Perez-Iratxeta, C., Andrade-Navarro, M. A. and Laprise, C. (2008). Genes to diseases (G2D) computational method to identify asthma candidate genes. *PLoS ONE* 3, e2907. doi:10.1371/journal.pone.0002907

Van Den Dries, K., Meddens, M. B. M., De Keijzer, S., Shekhar, S., Subramaniam, V., Figdor, C. G. and Cambi, A. (2013). Interplay between myosin IIA-mediated contractility and actin network integrity orchestrates podosome composition and oscillations. *Nat. Commun.* 4, 1412. doi:10.1038/ncomms2402

Van Goethem, E., Poincloux, R., Gauffre, F., Maridonneau-Parini, I. and Le Cabec, V. (2010). Matrix architecture dictates three-dimensional migration modes of human macrophages: differential involvement of proteases and podosome-like structures. *J. Immunol.* 184, 1049-1061. doi:10.4049/jimmunol.0902223

Van Goethem, E., Guiet, R., Balor, S., Charrière, G. M., Poincloux, R., Labrousse, A., Maridonneau-Parini, I. and Le Cabec, V. (2011). Macrophage podosomes go 3D. *Eur. J. Cell Biol.* **90**, 224-236. doi:10.1016/j.ejcb.2010.07.011

Van Helden, S. F. G., Oud, M. M., Joosten, B., Peterse, N., Figdor, C. G. and Van Leeuwen, F. N. (2008). PGE2-mediated podosome loss in dendritic cells is dependent on actomyosin contraction downstream of the RhoA-Rho-kinase axis. *J. Cell Sci.* **121**, 1096-1106. doi:10.1242/jcs.020289

Wabakken, T., Hauge, H., Funderud, S. and Aasheim, H.-C. (2002). Characterization, expression and functional aspects of a novel protein tyrosine phosphatase epsilon isoform. *Scand. J. Immunol.* **56**, 276-285. doi:10.1046/j.1365-3083.2002.01127.x

Wynn, T. A., Chawla, A. and Pollard, J. W. (2013). Macrophage biology in development, homeostasis and disease. *Nature* **496**, 445-455. doi:10.1038/nature12034

Xue, J., Schmidt, S. V., Sander, J., Draffehn, A., Krebs, W., Quester, I., De Nardo, D., Gohel, T. D., Emde, M., Schmidleithner, L. et al. (2014). Transcriptome-based network analysis reveals a spectrum model of human macrophage activation. *Immunity* **40**, 274-288. doi:10.1016/j.immuni.2014.01.006

Yu, C.-H., Rafiq, N. B. M., Krishnasamy, A., Hartman, K. L., Jones, G. E., Bershadsky, A. D. and Sheetz, M. P. (2013). Integrin-matrix clusters form podosome-like adhesions in the absence of traction forces. *Cell Rep.* **5**, 1456-1468. doi:10.1016/j.celrep.2013.10.040

Zasłona, Z., Przybranowski, S., Wilke, C., Van Rooijen, N., Teitz-Tennenbaum, S., Osterholzer, J. J., Wilkinson, J. E., Moore, B. B. and Peters-Golden, M. (2014). Resident alveolar macrophages suppress, whereas recruited monocytes promote, allergic lung inflammation in murine models of asthma. *J. Immunol.* **193**, 4245-4253. doi:10.4049/jimmunol.1400580
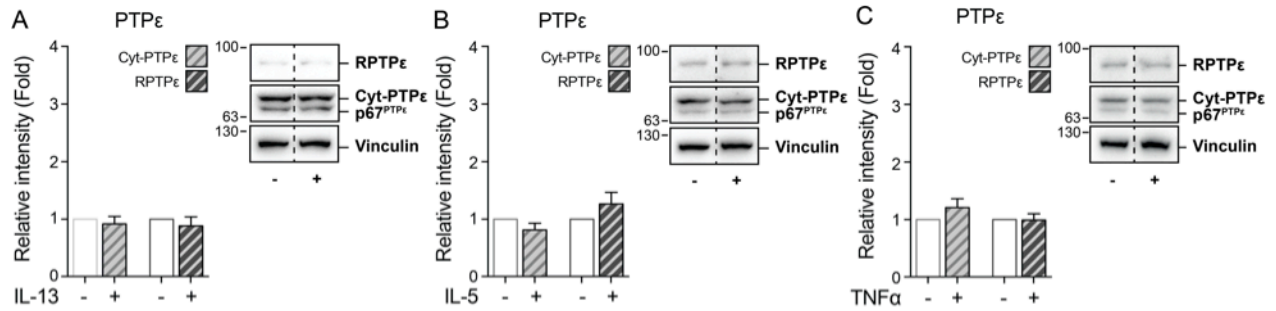
Figure S1. *Effect of Th1 and Th2 cytokines on PTPε isoform expression.* Human primary monocytes were stimulated with (A) IL-13 (20 ng/mL), (B) IL-5 (15 ng/mL), and (C) TNFα (10 ng/mL), for 24 hours. Cyt-PTPε and RPTPε protein expression was analyzed by western blot densitometry and expressed as relative intensity corrected for vinculin expression. Representative western blots are shown and the dotted lines indicate that the image of the membrane has been modified to remove lanes irrelevant to the result (A: n = 7, B: n = 7, C: n = 6). Data are expressed as mean ± s.e.m.
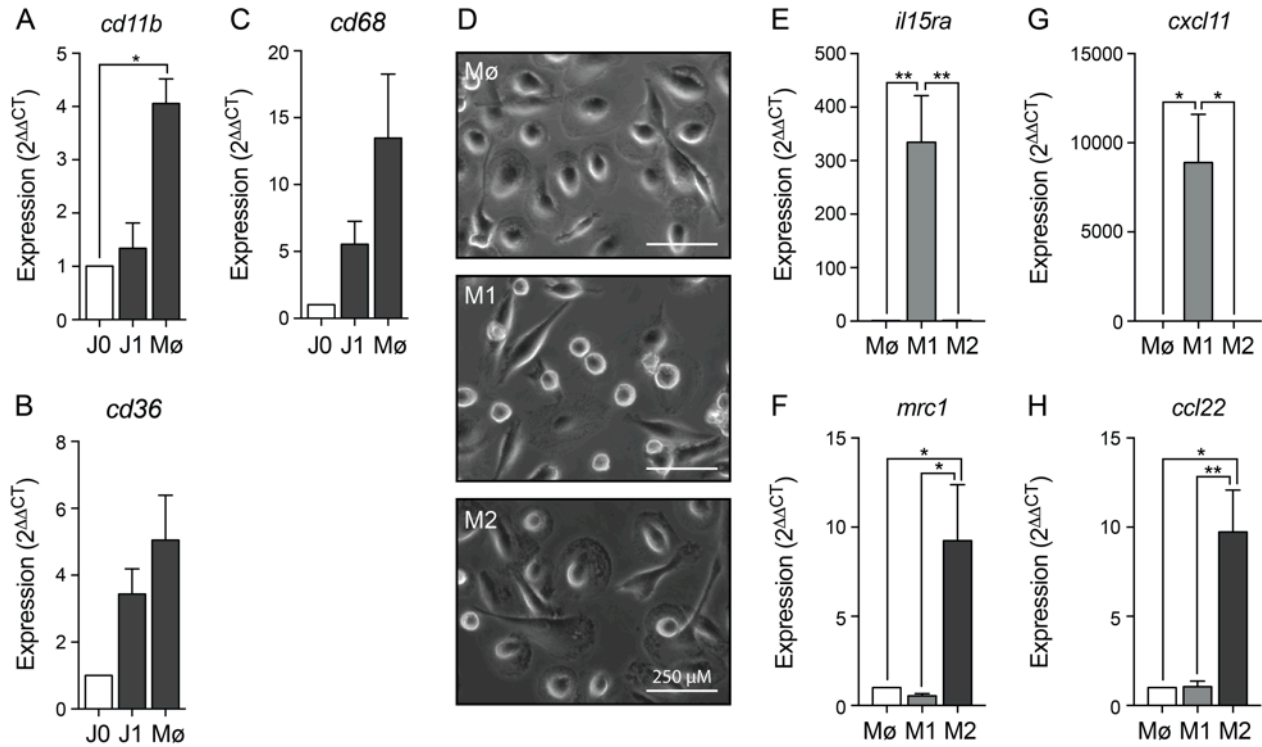
Figure S2. *Characterisation of hMDMs.* Human primary monocytes were differentiated according to the described protocol and mRNA expression of differentiation markers was analyzed by RT-qPCR and expressed as $2^{\Delta\Delta CT}$ over RPL13A mRNA expression ((A) *CD11b*, n = 3; (B) *CD36,* n = 3; (C) *CD68*, n =3). hMDMs were differentiated and polarized, as described in the experimental procedures section. For the resulting Mø, M1- and M2- polarized hMDMs, (D) photographs of representative hMDMs were taken with a Leica DM-IRBE inverted microscope and (E-H) differentiation marker mRNA expression was analyzed by RT-qPCR and expressed as $2^{\Delta\Delta CT}$ over RPL13A mRNA expression (n = 10- 11). The following primers were used:

cd11b_forward 5'-GCTGCCGCCATCATCTTAC-3'
cd11b_reverse 5'-CCACATGCCAGTGTTCTGC-3'
cd36_forward 5'-AGTTCTCAATCTGGCTGTGG-3'
cd36_reverse 5'-CGGAACCAAACTCAAAAATG-3'
cd68_forward 5'-CTAGCTGGACTTTGGGTGAGG-3'
cd68_reverse 5'-TCTCTGTAACCGTGGGTGTC-3'
il15ra_forward 5'-AGACAACAGCCAAGAACTGG-3',
il15ra_reverse 5'-TTGCCTTGACTTGAGGTAGC-3',
mrc1_forward 5'-GATAAACCCTGGGCCATGAG-3',
mrc1_reverse 5'-TTCTGTGATTCGGCATCCTG-3',
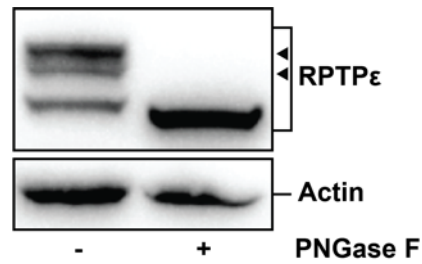
cxcl11_forward 5'-TGGGGTAAAAGCAGTGAAAG-3',

cxcl11_reverse 5'-TATAAGCCTTGCTTGCTTCG-3',

ccl22_forward 5'-TGATTACGTCCGTTACCGTC-3',

ccl22_reverse 5'-CCTGAAGGTTAGCAACACCAC-3'.

Data are expressed as mean ± SEM. * = $p < 0.05$, ** = $p < 0.005$ by one-way Anova with Tukey's multiple comparisons post-test.

Figure S3. *RPTPε presents multiple glycosylated forms.* HEK-LT1 cells were transiently transfected with RPTPε. Forty-eight hours post-transfection, cells were lysed and 80 μg of cell lysate was treated with PNGase F using the GlycoprofileTM II, Enzymatic In-Solution N-Deglycosylation Kit (PP0201, Sigma-Aldrich®); 5 enzymatic units for 1 hour at 37 °C. Western Blot illustrates RPTPε glycosylated forms. Arrows indicate glycosylated protein.
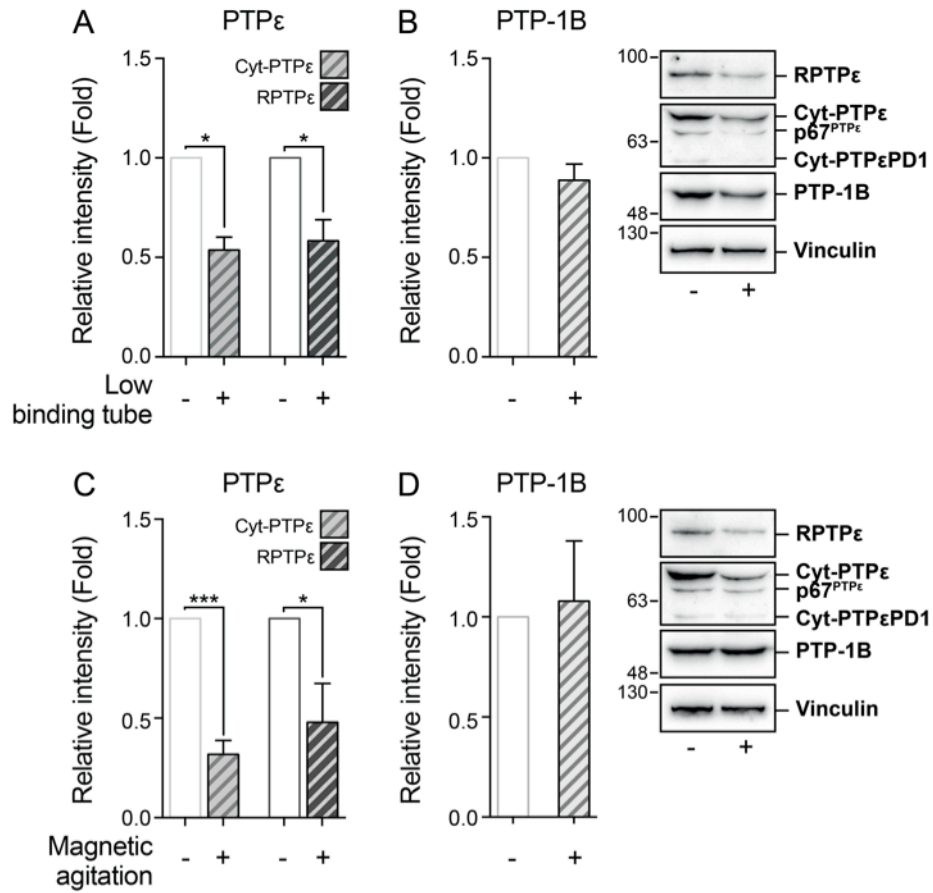
Figure S4. *Inhibition of adhesion prevents upregulation of PTPε expression*. Human primary monocytes were incubated overnight either in (A – B) low-binding plastic tubes (n = 3) or with (C – D) constant agitation (n = 5)). Expression of cyt-PTPε and RPTPε as well as of PTP-1B was then analyzed by western blot densitometry and expressed as relative intensity corrected for vinculin expression. Representative western blots are shown. Data are expressed as mean ± SEM. * = p < 0.05, *** = p < 0.001, by paired Student's t test.
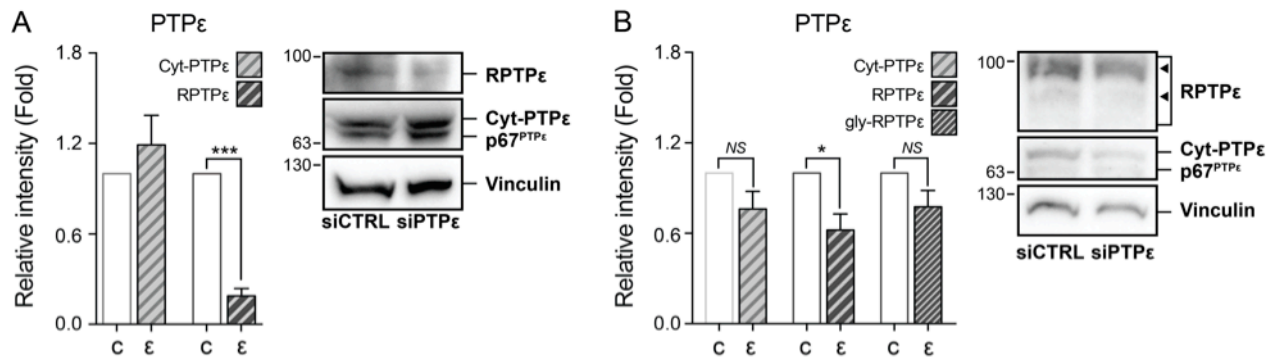
Figure S5. *Downregulation of RPTPε expression in human primary monocytes and M2- polarized hMDMs with siRNAs.* (A) Following a 48-hour incubation after siRNA (siCTRL: c, or siPTPε: ε) transfection in human primary monocytes (n = 4) or (B) following the transfection of siRNAs on days 5th and 7th – 3 hours before polarization – in M2-polarized hMDMs (n = 5), PTPε isoform expression was analyzed by western blot densitometry and expressed as relative intensity over vinculin expression. Representative western blots are shown. Data are expressed as mean ± SEM. * = p < 0.05, *** = p < 0.001, by paired Student's t test. Arrows indicate glycosylated protein.
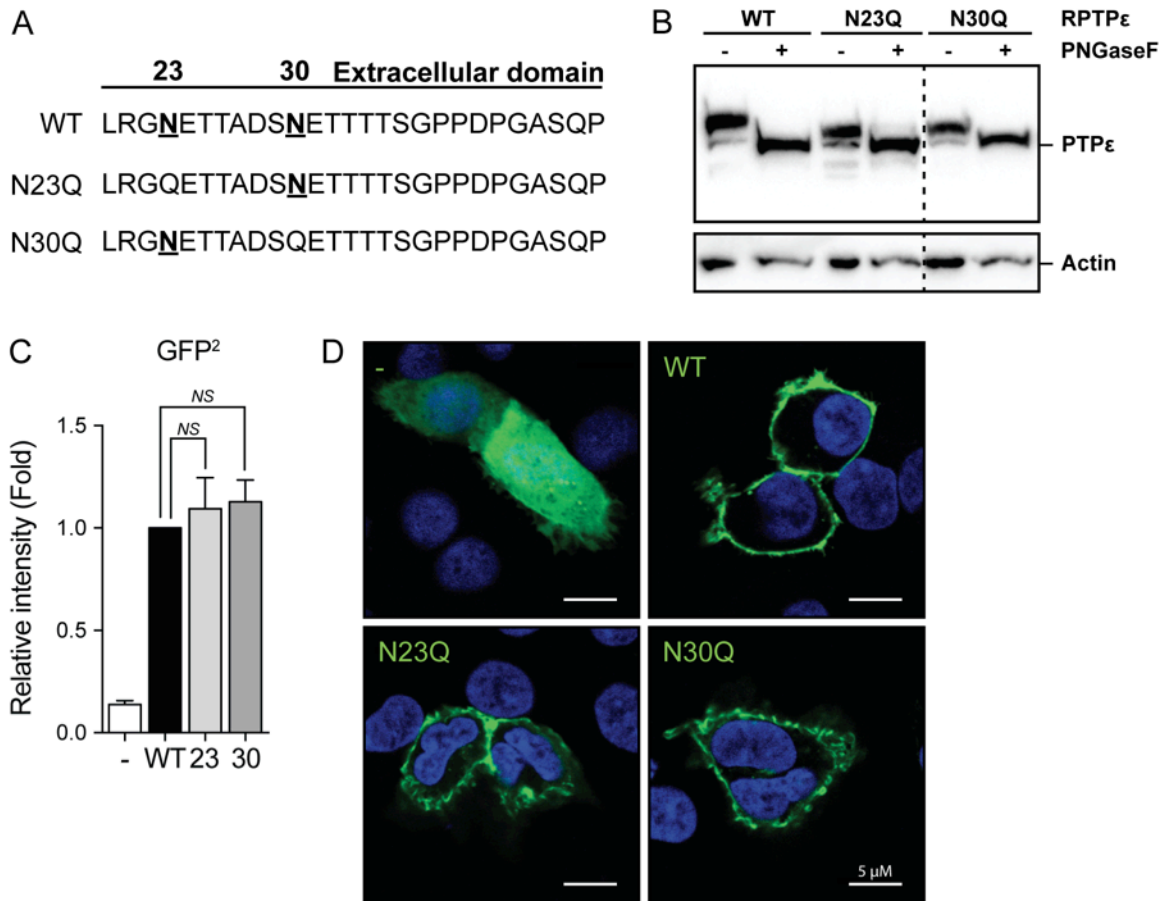
Figure S6. *Mutation of the asparagine extracellular residues of RPTPε decreases its glycosylation but does not affect the cellular localization and expression of the phosphatase in HEK-LT1.* (A) The first (N23) and second (N30) extracellular asparagine residues of RPTPε were mutated to glutamine (N23Q, N30Q), as described in the experimental protocol section, (B) decreasing their glycosylation levels as determined by western blot. A PNGaseF treatment further decreased the levels of residual glycosylation from the remaining residue. The dotted line indicates cropping within the same membrane. (C) cDNA constructs were expressed at the same levels, as shown by FACS, and (D) reached the cell membrane, as determined by laser scanning confocal microscopy. Representative images are shown.